Translational Oncology 57 (2025) 102402

Contents lists available at ScienceDirect

Translational Oncology

journal homepage: www.elsevier.com/locate/tranon

Investigating the molecular mechanisms and clinical potential of APO+ endothelial cells associated with PANoptosis in the tumor microenvironment of hepatocellular carcinoma using single-cell sequencing data

Zhaorui Cheng [a,b,1], Xiangyu Yang [e,1], Yi Ren [f,1], Huimin Wang [c], Qi Zhang [d], Sailing Lin [d], Wenhao Wu [d], Xiaolu Yang [d], Jiahan Zheng [g], Xinzhu Liu [d], Xin Tao [h], Xiaoyong Chen [d,*], Yuxin Qian [a,b,*], Xiushen Li [c,d,*]

[a] Department of Emergency, The Eighth Affiliated Hospital of Sun Yat-sen University, Shenzhen, Guangdong, China
[b] Department of Urology, The Eighth Affiliated Hospital of Sun Yat-sen University, Shenzhen, Guangdong, China
[c] Department of Traditional Chinese Medicine, Jiangxi Maternal and Child Health Hospital, Nanchang, Jiangxi, China
[d] Shenzhen University Medical School, Shenzhen University, Shenzhen, Guangdong, China
[e] Department of Gastroenterology and Hepatology, The Second Affiliated Hospital of Chongqing Medical University, Yuzhong District, Chongqing, China
[f] Southern University of Science and Technology, Shenzhen, Guangdong, China
[g] The First Clinical College, Gannan Medical University, Ganzhou, Jiangxi, China
[h] Department of Pathology, Second Affiliated Hospital of Nanchang University, Nanchang, JiangXi, China

ARTICLE INFO

Keywords:
Hepatocellular carcinoma
PANoptosis
Tumor microenvironment (TME)
Endothelial cells
Immunotherapy

ABSTRACT

Introduction: PANoptosis is a newly identified form of programmed cell death that integrates elements of pyroptosis, apoptosis, and necroptosis. It plays a pivotal role in shaping the tumor immune microenvironment. Despite its significance, the specific functions and mechanisms of PANoptosis within the tumor microenvironment (TME) of hepatocellular carcinoma (HCC) remain unclear. This study aims to investigate these mechanisms using single-cell RNA sequencing data.

Methods: Single-cell RNA sequencing data from HCC patients were obtained from the GEO database. The AUCell algorithm was used to quantify PANoptosis activity across various cell types in the TME. Cell populations with high PANoptosis scores were further analyzed using CytoTRACE and scMetabolism to assess their differentiation states and metabolic profiles. Associations between these high-score cell subsets and patient prognosis, tumor stage, and response to immunotherapy were examined. Cell-cell communication analysis was performed to explore how PANoptosis-related APO+ endothelial cells (ECs) may influence HCC progression. Immunofluorescence staining was used to assess the spatial distribution of APO+ ECs in tumor and adjacent tissues. Finally, a CCK8 assay was conducted to evaluate the effect of APOH+ HUVECs on HCC cell proliferation.

Results: A total of 16 HCC patient samples with single-cell RNA sequencing data were included in the study. By calculating the PANoptosis scores of different cell types, we found that ECs, macrophages, hepatocytes, and fibroblasts exhibited higher PANoptosis scores. The PANoptosis scores, differentiation trajectories, intercellular communication, and metabolic characteristics of these four cell subpopulations with high PANoptosis scores were visualized. Among all subpopulations, APO+ ECs demonstrated the most significant clinical relevance, showing a positive correlation with better clinical staging, prognosis, and response to immunotherapy in HCC patients. Cellular communication analysis further revealed that APO+ ECs might regulate the expression of HLA molecules, thereby influencing T cell proliferation and differentiation, potentially contributing to improved prognosis in HCC patients. Immunofluorescence staining results indicated that APO+ ECs were primarily located in the adjacent tissues of HCC patients, with lower expression in tumor tissues. The results of cellular experiments showed that APOH+ HUVECs significantly inhibited the proliferation of HCC cells.

* Corresponding authors.
E-mail addresses: czr168756179@163.com (Z. Cheng), xiangyu_yang_23@163.com (X. Yang), 13340907185@163.com (Y. Ren), basschen99@163.com (X. Chen), qianyuxin96@163.com (Y. Qian), lixiushenzplby@163.com (X. Li).
[1] These authors contributed equally to this work.

https://doi.org/10.1016/j.tranon.2025.102402
Received 24 February 2025; Received in revised form 27 March 2025; Accepted 19 April 2025

Conclusions: This study systematically mapped the cellular landscape of the TME in HCC patients and explored the differences in differentiation trajectories, metabolic pathways, and other aspects of subpopulations with high PANoptosis scores. Additionally, the study elucidated the potential molecular mechanisms through which APO+ ECs inhibit HCC cell proliferation and improve prognosis and immunotherapeutic efficacy in HCC patients. This research provides new insights for clinical prognosis evaluation and immunotherapy strategies in HCC.

Introduction

Hepatocellular carcinoma (HCC), the most common form of primary liver cancer [1], is the third leading cause of cancer-related deaths globally [2]. Surgical intervention is the primary treatment for early-stage HCC, while immunotherapy is more commonly employed in advanced stages [3,4]. However, high rates of postoperative recurrence and immune resistance pose significant challenges in the clinical management of HCC, adversely affecting patient prognosis and quality of life [5,6]. This underscores the need for deeper exploration of HCC's molecular biology to identify novel insights that could improve therapeutic outcomes.

PANoptosis is a coordinated programmed cell death (PCD) mechanism that integrates pyroptosis, apoptosis, and necroptosi [7]. As an inflammatory type of PCD, PANoptosis can be induced by tumor necrosis factor (TNF) and interferon-gamma (IFN-γ), potentially triggering a cytokine storm [8,9]. It can synergistically eliminate tumor cells through multiple cell death pathways while activating anti-tumor immune responses, thus holding significant potential in cancer therapy [10,11]. Cai et al. [12] found that glioma patients with high PANoptosis enrichment scores showed significantly enhanced immune sensitivity. Moreover, PANoptosis-targeting drugs combined with anti-PD-1 therapy demonstrated a strong synergistic effect in glioma models. In HCC, tumor cells with high DNASE1L3 expression induce PANoptosis through activation of the melanoma 2 pathway, thereby promoting the activation of anti-tumor immunity [13]. However, the relationship between PANoptosis and the TME in HCC remains inadequately understood. An in-depth multi-omics analysis of the role of PANoptosis in the TME of HCC is expected to provide new strategies for clinical treatment of HCC patients.

Tumor microenvironment (TME) of HCC plays a pivotal role in influencing treatment responses and prognosis [14]. The TME is composed of tumor cells alongside various interacting cell types, including immune and stromal cells, such as tumor-associated macrophages (TAMs) [15], cancer-associated fibroblasts (CAFs) [16] and tumor endothelial cells (ECs) [17]. These cell types are intimately involved in tumor progression, invasion, and metastasis [18]. Specific subtypes of TME cells are strongly linked to therapeutic outcomes in cancer. For instance, macrophages, the most prevalent immune cells in the TME, contribute to tumor progression through mechanisms like angiogenesis and cancer cell remodeling [19]. CAFs support immune evasion through multiple pathways [20], while ECs promote angiogenesis and tumor metastasis [21]. Despite these insights, the precise role of these cellular clusters in the PANoptosis process within HCC remains unclear. Therefore, unraveling the interactions among different cell types in the TME is essential for advancing both scientific understanding and clinical treatment strategies for HCC.

In this study, we systematically constructed a cellular atlas of the TME in HCC patients by analyzing single-cell RNA sequencing (scRNA-seq) data. We also computed the PANoptosis scores for each cell type. We further explored the differences in developmental trajectories, metabolic pathways, and gene expression profiles of cells with high PANoptosis scores. Notably, APO+ ECs were closely associated with better clinical staging, prognosis, and immune therapy responses in HCC patients. This relationship likely relates to their regulation of T cell proliferation and differentiation through HLA. Experimental results demonstrated that APO+ ECs predominantly localize in adjacent non-tumor tissues rather than in the tumor tissues themselves and are capable of significantly inhibiting HCC cell proliferation. In conclusion, our findings suggest that APO+ ECs may play a critical role in modulating intercellular communication within the TME, influencing HCC development, progression, and immune evasion. This provides new insights and potential targets for clinical prognosis evaluation and immunotherapy in HCC.

Method

Experimental workflow

First, quality control and normalization were performed on the obtained single-cell RNA sequencing data to identify different cell types within the TME. Next, a PANoptosis score was calculated for each cell type, followed by differentiation trajectory and metabolic characteristic analysis for those cell types with high PANoptosis scores. To assess the prognostic value of the PANoptosis score, we further analyzed the correlation between high PANoptosis score subpopulations and clinical information from HCC patients. Subsequently, cell communication analysis was conducted to investigate the role of APO+ ECs in the TME, uncovering their molecular mechanisms in HCC initiation and progression. Immunofluorescence staining was used to evaluate the spatial distribution of APO+ ECs in tumor and adjacent non-tumor tissues from HCC patients. Finally, an APO+ ECs-HCC cell co-culture model was established to observe the effects of APO+ ECs on the proliferation, migration, and invasion of HCC cells. The overall experimental workflow is illustrated in Fig. 1.

Data sources

The study included scRNA-seq data from 16 HCC patients, retrieved from the Gene Expression Omnibus (GEO) database (https://www.ncbi.nlm.nih.gov/geo/). These data were sourced from three datasets: GSE149614 (10 HCC patients), GSE166635 (2 HCC patients), and GSE189903 (4 HCC patients).Furthermore, we utilized The Cancer Genome Atlas (TCGA) database (https://www.cancer.gov/ccg/research/genome-sequencing/tcga), specifically the TCGA-LIHC dataset, which includes extensive RNA sequencing data and clinical information from 377 HCC patients.

Identification of cell types within the TME

We processed scRNA-seq data using the Seurat package in R (version 4.4.1). Initially, a Seurat object was constructed, and data preprocessing was performed based on the following filtering criteria: removal of cells with fewer than 200 or >5000 RNA features, and cells with mitochondrial gene expression exceeding 10 %. The data were normalized using the NormalizeData function and subsequently standardized using the ScaleData function. Principal Component Analysis (PCA) was then performed using the RunPCA function, with the first 10 principal components selected to reduce the dimensionality of the data. To address batch effects, we applied the Harmony algorithm for batch integration. Further dimensionality reduction was performed using the RunUMAP function for visualization. A total of 16 distinct cell clusters were identified based on the UMAP results. To accurately annotate the cell types within the TME of HCC, we utilized the SingleR package for cell cluster annotation, and the FindAllMarkers function was employed to validate marker genes for each identified cell type. Ultimately, we identified nine

major cell types within the TME of HCC.

Cell-Cell communication analysis in the TME

To explore the cellular interactions within the TME of HCC, we performed a cell-cell communication analysis using the CellChat R package (version 1.5.0). Initially, we constructed a CellChat object using the createCellChat function to facilitate further analysis. Subsequently, potential ligand-receptor interactions between nine major cell types were identified through the CellChat database. The communication results were aggregated using the aggregateNet function, systematically revealing the cellular communication pathways. For quantitative analysis and visualization of the communication network, we employed the netVisual_circle function to generate network diagrams, illustrating the quantity and strength of interactions between different cell types. Additionally, we utilized the netAnalysis_computeCentrality function to analyze the input and output weights of various signaling pathways, thereby quantifying their significance in the communication process. Through these methods, we constructed a comprehensive network of molecular interactions among cells within the TME of HCC.

PANoptosis scores of cell subpopulations within the TME

The PANoptosis-related gene sets used in this study were derived from multiple published papers [10,22,23], and these gene sets have been widely referenced in various studies, thus providing reliable reference sources (please see the citations). For the evaluation of gene set activity scores, we utilized the AUCell analysis method. Specifically, the AUCell analysis first ranks all genes in each cell according to their expression levels, creating a gene ranking list, where genes with higher expression are ranked higher. Then, for each gene in the gene set, we find its position in the gene ranking list of each cell, which reflects the expression intensity of genes within the gene set in a specific cell population. Subsequently, based on the ranking of the genes in each cell, we calculated the activity score of the gene set. The score is calculated using the Area Under the Curve (AUC) method, which reflects the cumulative area based on the gene rankings. The larger the AUC value, the higher the expression activity of that gene set in the specific cell. The size of the AUC value indicates the overall activity level of the gene set in the cell population.To precisely calculate the activity score of the pan-apoptosis-related genes, we first used the AUCell_buildRankings function to rank the genes in the expression matrix, and then extracted the pan-apoptosis-related genes from the ranking results for further analysis. Finally, by calculating the activity score of the pan-apoptosis-related gene set in each cell population, we obtained the pan-apoptosis score for each cell group, providing a quantitative measure for studying the pan-apoptosis process.

Pseudotime analysis of cell subpopulations within the TME

In the analysis of developmental trajectories for TME cells, we utilized the Monocle package (version 2.4.0) to explore the developmental pathways of various TME cell subgroups in HCC. We began by scaling, normalizing, and clustering the scRNA-seq data using the Seurat tool, and then loaded this data into a Monocle object. Differentially expressed genes were identified for each cluster using the DifferentialGeneTest function. We plotted the cellular developmental trajectories and further analyzed differentially expressed genes over pseudotime using the same function. Finally, we generated a heatmap using the plot_pseudotime_heatmap function to visualize changes in the top 100 genes

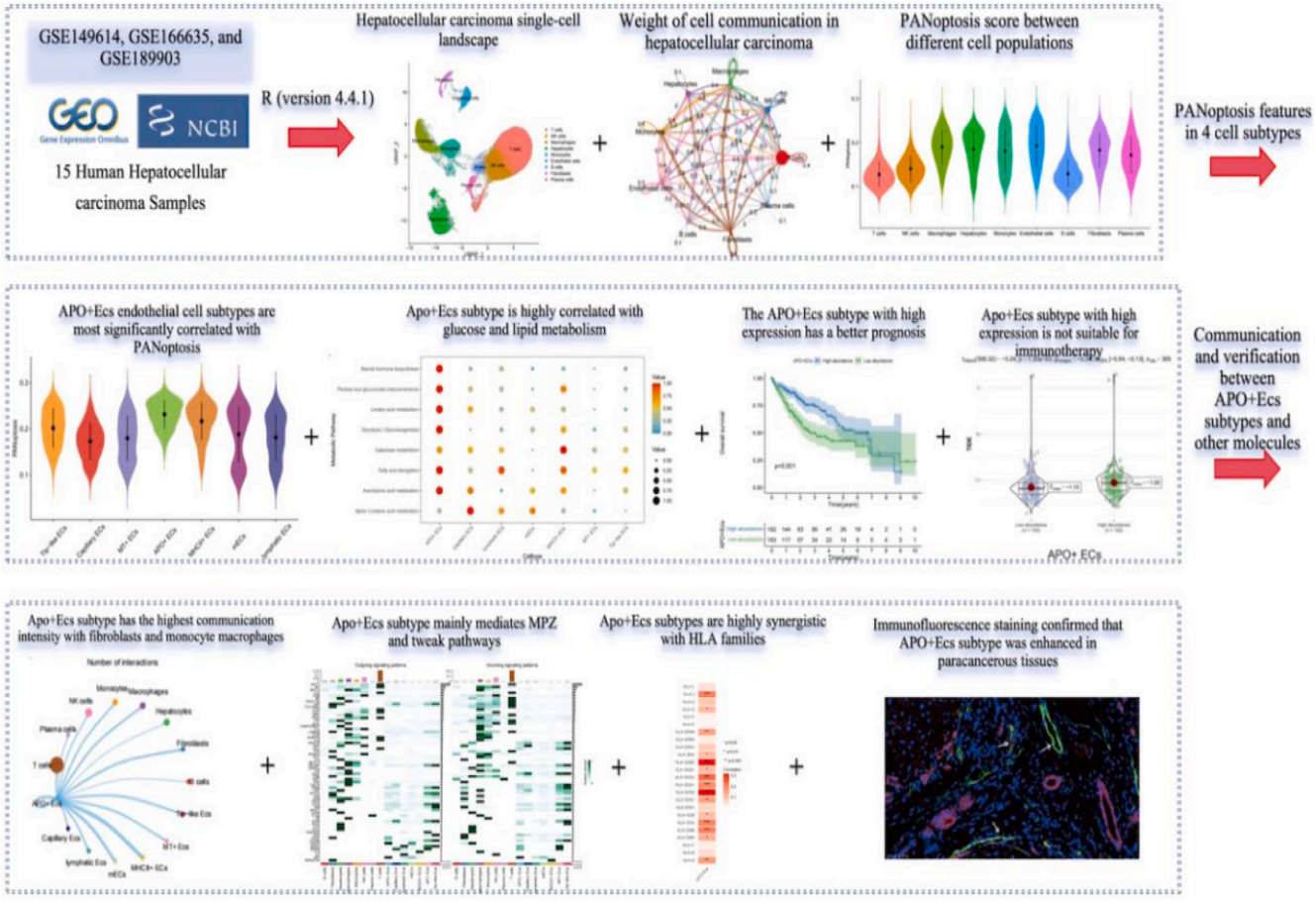

Fig. 1. Flow Chart.

with the most significant differential expression across pseudotime.

Assessment of differentiation potential of cell subpopulations

We employed the CytoTRACE software package to assess the differentiation potential and status of various cell subpopulations. Unlike traditional lineage trajectory analysis methods, CytoTRACE predicts the relative differentiation state and direction of cells without relying on specific time scales or continuous developmental processes. In this analysis, we first calculated the stemness score for each cell using the CytoTRACE function, which reflects its undifferentiated state. A higher stemness score indicates that a cell is closer to an undifferentiated or early differentiation stage. To visualize the results, we utilized the plotCytoTRACE function to present the relationship between stemness scores and spatial distribution of cells, thereby revealing the differentiation potential and spatial characteristics of the distinct cell subpopulations.

Metabolic analysis of cell subpopulations

We conducted a comprehensive analysis of the metabolic characteristics of cell subpopulations obtained through secondary clustering using the scMetabolism R package. Initially, we assessed the activity of 85 metabolic pathways from the KEGG database across different cell subpopulations by combining AUCell scores with the sc.metabolism. Seurat function. This analysis provided a quantitative representation of the metabolic activity in each subpopulation, allowing for a more precise understanding of their metabolic profiles. To further explore the differences in metabolic pathways across the cell subpopulations, we visualized key metabolic pathways, including carbohydrate metabolism and lipid metabolism, using bubble plots.

Transcription factor analysis of cell subpopulations

In this study, we performed transcriptional regulatory network analysis based on the hg38 database provided by RcisTarget (version 1.6.0) using the default parameters of the SCENIC algorithm (version 1.1.2.2). The SCENIC algorithm identifies potential transcription factors and their target genes, thereby inferring transcriptional regulatory networks at the single-cell level, which helps to reveal the regulatory roles of transcription factors in different cell subpopulations. To assess the activation state of transcription factors, we employed a non-binary classification method to quantify their activation or inhibition in various cell subgroups. Subsequently, we used the ComplexHeatmap package in R to visualize the activation status of regulons, which are composed of transcription factors and their regulated genes.

Survival analysis and immunotherapy analysis of PANoptosis-Related cells based on bulk RNA data

We identified four TME cell subtypes most closely associated with PANoptosis. Next, we constructed cell scores based on the top 100 differentially expressed genes for each subtype and assessed their cellular proportions using the ssGSEA function. To investigate the effect of cellular abundance on prognosis, we performed survival analysis and plotted survival curves using the survival and survminer packages in R. Furthermore, we analyzed the Bulk RNA data from TCGA-LIHC using the TIDE website (http://tide.dfci.harvard.edu/) to explore the potential impact of PANoptosis on the effectiveness of immunotherapy. Finally, the results were visualized using the ggplot2 and ggstatsplot R packages.

Immunofluorescence (IF) staining

Formalin-fixed paraffin-embedded (FFPE) tissues from three HCC patients were collected from the Second Affiliated Hospital of Nanchang University. These samples included both tumor tissues and corresponding adjacent non-tumor tissues. The study protocol was approved by the Research Ethics Committee of the Second Affiliated Hospital of Nanchang University (Ethical Approval Number: O-2024,147). Paraffin was removed from the FFPE tissue sections using xylene. The sections were then sequentially immersed in 100 %, 95 %, 85 %, and 70 % ethanol for 5 min each and subsequently washed with distilled water. After heating the sections at 98 °C in 10 mM citrate buffer, they were allowed to cool to room temperature and then rinsed three times with phosphate-buffered saline (PBS) for 5 min each. The sections were incubated with 10 % goat serum for 30 min and then with CD31 (1:200) overnight in a humid chamber at 4 °C. After washing with PBS, the sections were incubated with fluorescently labeled secondary antibodies for 60 min at room temperature. Following another wash, additional antibodies (APOH, TTR, RGCC) were applied overnight at 4 °C in a humid chamber. Secondary antibodies were used as previously described. Finally, the samples were stained with DAPI for 10 min to visualize nuclei and then mounted in a containment solution. Observations and photography were performed using a fluorescence microscope.

Establishment of co-culture model

To establish the co-culture model, HUVEC transfected with either the control plasmid or the APOH overexpression plasmid were co-cultured with HCC cell lines (HCCLM3 and Huh7) at a 3:1 ratio. Specifically, HUVEC cells were seeded in the lower chamber, while the HCC cells were seeded in the upper chamber of Transwell inserts. After 48 hours of co-culture, HCC cells were collected to assess alterations in their proliferation, migration, and invasion capabilities.

Cell culture and transfection

HCC cell (HCCLM3 and Huh7), along with HUVEC, were obtained from Shanghai Fuheng Cell Biology Co., Ltd. All cell lines were cultured under standard conditions. The corresponding culture media were replaced regularly based on the specific requirements of each cell line to ensure optimal cell growth conditions. For the overexpression of APOH, cells were transfected with the APOH overexpression plasmid was designed and synthesized by (Beijing Tsingke Biotech Co., Ltd.) using the Lipo8000(beyotime) transfection reagent, according to the manufacturer's protocol.

Quantitative real-time PCR (qRT-PCR)

HUVEC cells were collected 48 hours after APOH overexpression plasmid transfection. The experiment was conducted according to the instructions provided with the reagent kits. First, total RNA was extracted from the cells using the RNAisoPlus reagent kit (Takara, 9108/9109, Japan). Next, mRNA was reverse transcribed into cDNA using the PrimeScript RT reagent kit (Takara, RR037A, Japan). Real-time quantitative PCR amplification was then performed using the TB Green Premix Ex Taq II reagent kit (Takara, RR820A, Japan). GAPDH was used as an internal control for normalization, and relative mRNA expression levels of the target genes were calculated using the 2-ΔΔCt method. APOH primer sequences were designed and synthesized by (Guangzhou IGE Biotechnology Co., Ltd.)the sequences are as follows:

APOH-F: 5′-CTCTATCGGGACACAGCAGTTTTT-3′;
APOH-R: 5′-ATTGTCTGGTCTTGATGGGAATGG-3′;
GAPDH-F: 5′-ACAGCCTCAAGATCATCAGCA-3′;
GAPHD-R: 5′-ATGAGTCCTTCCACGATACCA-3′;

CCK-8 cell proliferation assay

HCC cells (HCCLM3 and Huh7) co-cultured with HUVEC cells for 48 hours were seeded at a density of 3000 cells per well into a 96-well plate. The cells were then incubated at 37 °C in a 5 % CO_2 atmosphere. Proliferation was assessed at 24, 48, and 72 hours post-seeding by adding 10

μL of CCK-8 solution to each well, followed by a 2-hour incubation. Absorbance at 450 nm was measured using a microplate reader to determine the optical density values, which were used to evaluate cell proliferation.

Statistical analyses

All statistical calculations and graphs were performed using R software version 4.4.1. Kaplan-Meier curves and log-rank tests were utilized to examine differences in survival among various risk groups. A two-sided p-value of <0.05 was considered statistically significant.Statistical significance was defined as $*P < 0.05$, $**P < 0.01$, $***P < 0.001$.

Result

Cellular composition and PANoptosis features in the TME of HCC

We conducted integration and quality control of the data prior to analysis, ultimately retaining 27,443 normal control cells and 98,964 HCC cells, for a total of 126,407 cells used in subsequent analysis (Supplementary Figure 1A). Based on the JackStrawPlot and ElbowPlot results, we selected the first 10 principal components for dimensionality reduction and clustering (Supplementary Figures 1B-C). After batch effect correction, 16 distinct cell clusters were identified (Fig. 2A). Uniform Manifold Approximation and Projection visualization revealed an even distribution of cells across the three datasets, confirming the effectiveness of batch effect correction (Fig. 2B). Using existing literature data, we classified the clusters into nine cell types (Fig. 2C). These cell types and their associated markers include: T cells (CD2, CD3D, CD3E), NK cells (NKG7, GNLY), macrophages (CD163), hepatocytes

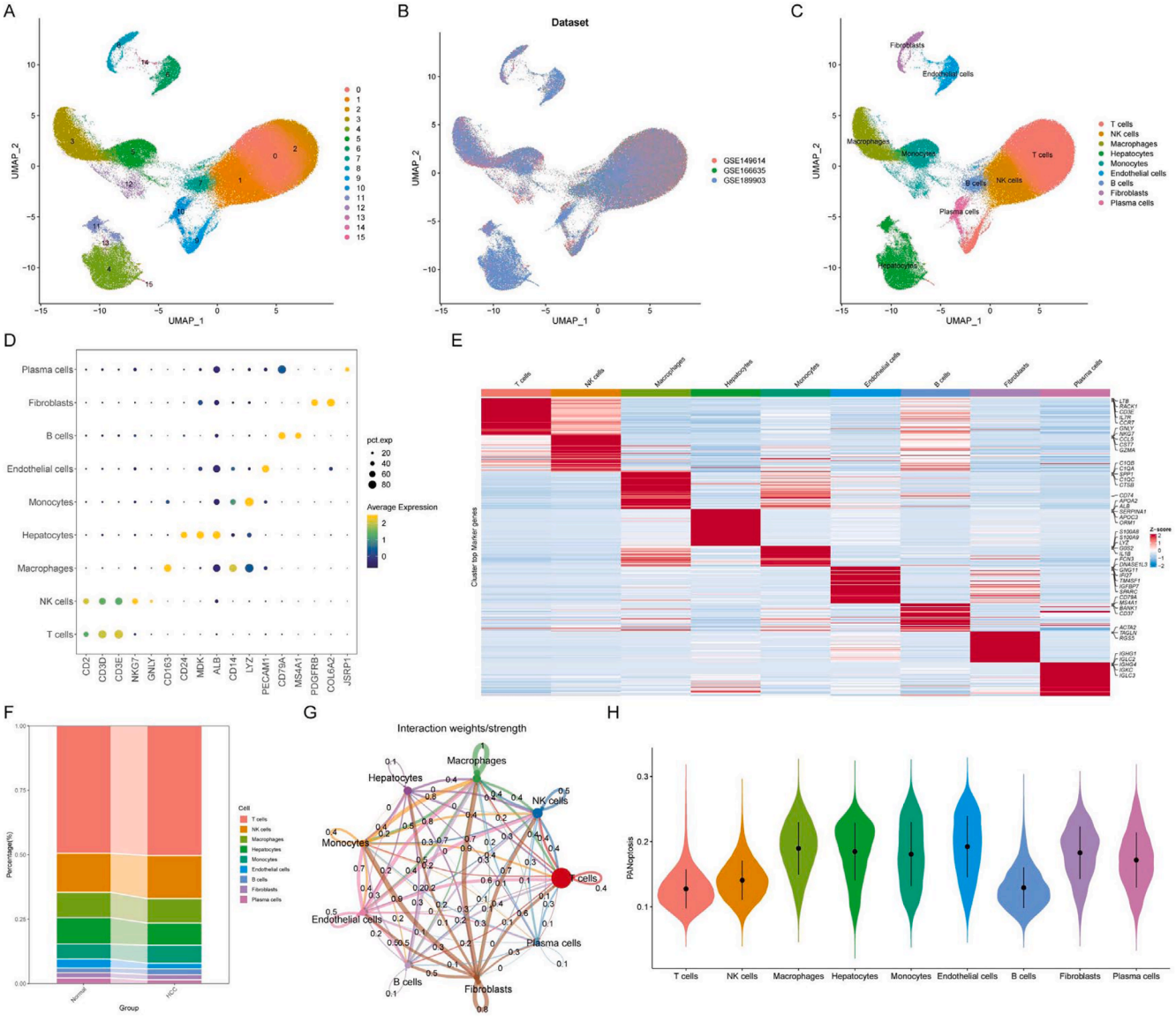

Fig. 2. Overview of the main cell types in hepatocellular carcinoma (HCC) single-cell data. (A) UMAP plot of the main cell populations in hepatocellular carcinoma. (B) Integration results of three single-cell RNA sequencing datasets collected from the Gene Expression Omnibus (GEO) database. (C) UMAP plot of the nine main cell lineages based on classical marker genes. (D) Bubble chart of the average expression of marker genes in the nine main cell lineages. (E) Heatmap showing the top 50 differentially expressed genes in the nine main cell lineages. (F) Differences in the proportions of the nine main cell lineages between normal and HCC groups. (G) Cell communication among the nine main cell lineages. (H) PANoptosis scores of the nine main cell lineages. *Note*: PANoptosis refers to a newly identified form of programmed cell death that integrates apoptosis, necroptosis, and pyroptosis.

(CD24, MDK, ALB), monocytes (CD14, LYZ), endothelial cells (PECAM1), B cells (CD79A, MS4A1), fibroblasts (PDGFR2, COL6A2), and plasma cells (JSRP1) (Fig. 2D). Further analysis of the top 50 differentially expressed genes for each cell type revealed that almost all marker genes were present in the list, supporting the high accuracy of our cell type annotation (Fig. 2E).

When comparing the cellular composition between the HCC and control groups, we observed a significant increase in the proportion of NK cells and monocytes in the HCC group, while the proportion of endothelial cells was significantly reduced (Fig. 2F). Cell-cell communication analysis revealed that fibroblasts send numerous signals to monocytes and macrophages, which may contribute to HCC initiation and progression (Fig. 2G). Pathway interaction analysis indicated heightened activation of chemotactic signaling pathways, such as MIF-CD74+CXCR4 and MIF-CD74+CD44, suggesting a highly chemotactic microenvironment in HCC (Supplementary Figure 1D). Using the AUCell algorithm to calculate PANoptosis scores, we found higher scores in ECs, macrophages, hepatocytes, and fibroblasts, while B cells exhibited the lowest scores (Fig. 2H). Based on these findings, we will further investigate the roles of ECs, macrophages, hepatocytes, and fibroblasts in HCC, focusing on the impact of PANoptosis in the disease.

Identification of hepatocyte subpopulations and their differentiation and metabolic characteristics

Hepatocytes exhibit distinct tissue-specific responses during HCC progression. Based on secondary clustering analysis, we categorized hepatocytes into 14 subpopulations (Supplementary Figure 2A). Annotation with marker genes further classified these hepatocytes into eight types: APOE+, HSP+, PAGE+, Ig+, inflammatory, GLUL+, MT+, and KRT+ hepatocytes (Fig. 3A, Supplementary Figure 2B). In HCC tumor tissues, the proportions of APOE+, HSP+, and GLUL+ hepatocytes were significantly increased, whereas PAGE+, inflammatory, and MT+ hepatocytes showed a significant decrease (Fig. 3B). The PANoptosis scores of different subpopulations revealed that Ig+ hepatocytes exhibited the highest PANoptosis score (Fig. 3C). Using the Monocle2 algorithm, we reconstructed the differentiation trajectory of hepatocyte subpopulations, which indicated that PAGE+ hepatocytes are in an early stage of differentiation, while inflammatory hepatocytes are likely in a later stage, consistent with the diffuse inflammation observed in advanced HCC (Fig. 3D-E). A pseudo-time heatmap of the top 100 genes revealed four distinct expression patterns: cluster 1 exhibited higher expression in the late stages, cluster 2 was highly expressed in the early stages, cluster 3 showed expression in the mid-stage, and cluster 4 was highly expressed in the late stages (Fig. 3F). Given the importance of metabolic processes in HCC, we further conducted a single-cell metabolic score analysis. The results indicated that APOE+ and MT+

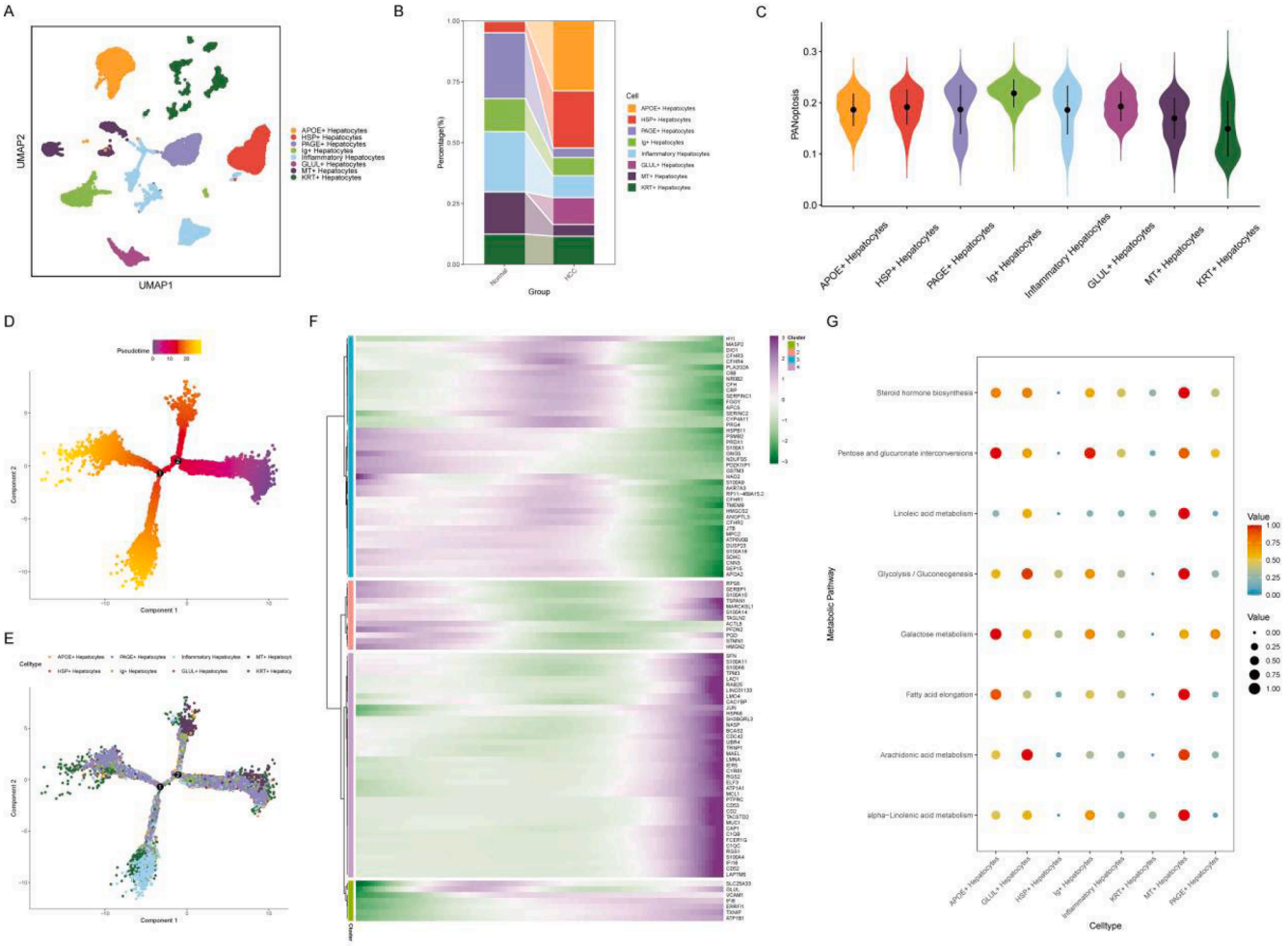

Fig. 3. Overview of major hepatocyte subtypes. (A) UMAP plot showing the subtypes of hepatocytes. (B) Differences in the proportions of hepatocyte subtypes between HCC and normal tissues. (C) PANoptosis scores of hepatocyte subtypes. (D-E) Pseudotime analysis of hepatocytes, a technique that orders single cells along a temporal axis to reflect their differentiation status. (F) Pseudotime gene heatmap of dynamic gene changes in hepatocytes. (G) Bubble chart of the differences in scores among different metabolic pathways for hepatocyte subtypes.

hepatocytes were in a high lipid metabolism state, while GLUL+ and MT+ hepatocytes demonstrated strong glycolytic activity. Additionally, Ig+, APOE+, and MT+ hepatocytes were associated with the Pentose and glucuronate interconversions. These results suggesting that metabolic regulation could be a potential target for HCC intervention (Fig. 3G). This study reveals the heterogeneity of hepatocyte subpopulations in HCC, elucidating their unique roles in PANoptosis, cellular differentiation, and metabolism pathways. These findings provide crucial insights into the pathogenesis of HCC and offer potential directions for novel therapeutic strategies.

Characterization of macrophage subpopulations in the TME of HCC

Macrophages exhibit the highest PANoptosis score among immune cells, prompting further investigation. Through secondary dimensionality reduction clustering, we identified eight macrophage subpopulations (Fig. 4A). Proportional analysis revealed a significant increase in the proportion of MMP12+ and MHCII+ SPP1+ macrophages in HCC samples, while the proportion of HSP+, MARCO+, Ig+, and APO+ macrophages decreased (Fig. 4B). MMP12 is associated with extracellular matrix remodeling, and MHCII molecules play a crucial role in antigen presentation. The increased presence of these macrophage subsets may contribute to TME remodeling and inflammation activation, both of which are recognized as critical drivers of tumor progression. PANoptosis score analysis indicated the highest score in MMP12+ macrophages and the lowest in monocyte-like macrophages (Fig. 4C). Pseudotime trajectory analysis further demonstrated that SPP1+ macrophages predominantly appeared in early differentiation stages, while MHCII+ macrophages dominated late stages of differentiation, suggesting a key role of MHCII+ macrophages in antigen presentation (Fig. 4D-E, Supplementary Figure 3A). However, whether these immune cells can effectively exert antitumor effects or merely promote an inflammatory microenvironment remains to be explored. Gene heatmap analysis of pseudotime progression revealed that genes in clusters 1 and 3 were primarily associated with mid-differentiation, cluster 2 with early differentiation genes, and cluster 4 with late-stage differentiation genes (Fig. 4F). To further investigate the transcriptional regulatory networks of macrophage subpopulations, we performed SCENIC analysis. This revealed that MACRO+ macrophages, which are highly associated with PANoptosis, express key transcription factors such as NFIA, TCF7L2, and IRF2. These factors may play crucial roles in the transcriptional regulation of PANoptosis-related genes (Fig. 4G, Supplementary Figure 3B-D).

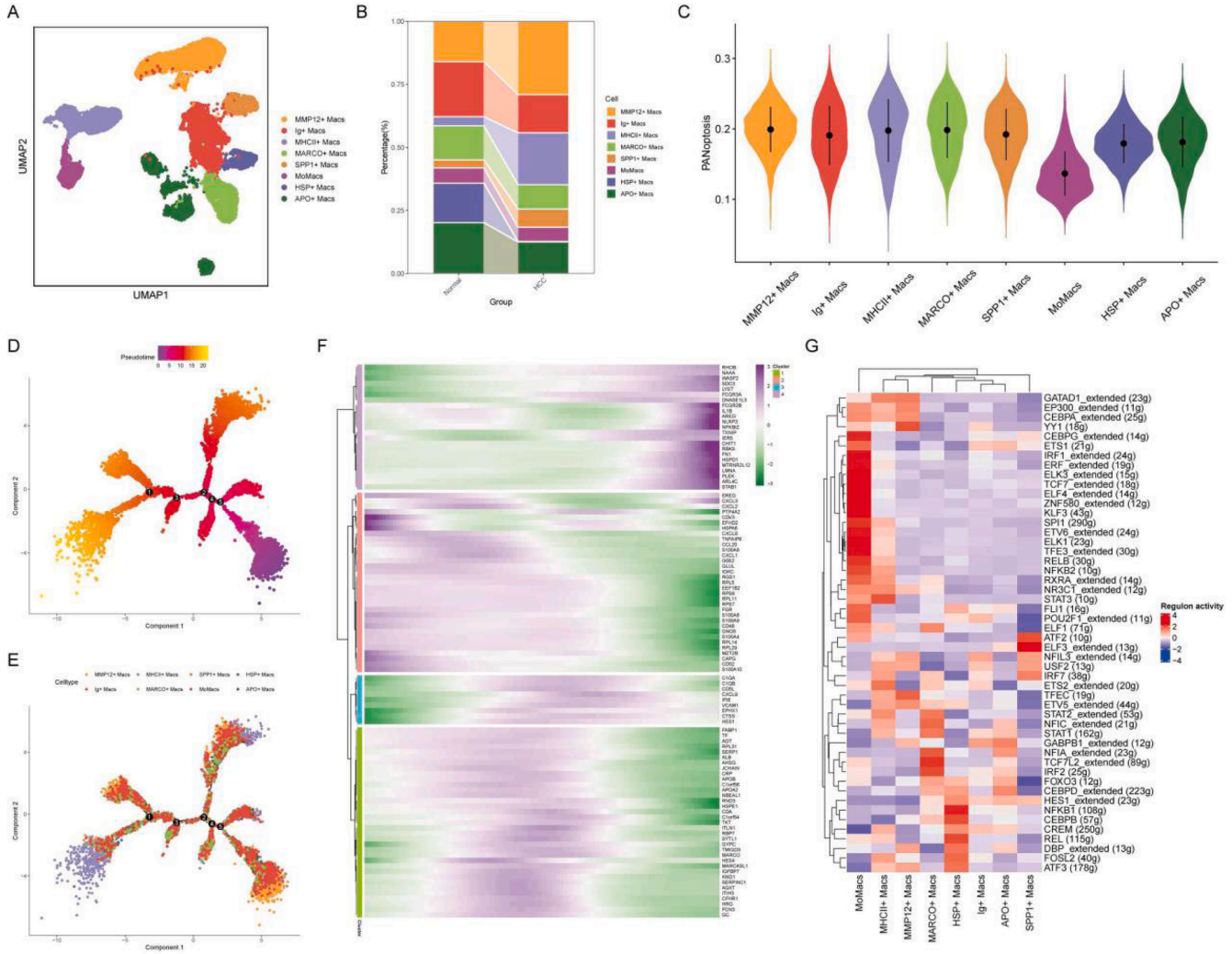

Fig. 4. Overview of major macrophage subtypes. (A) UMAP plot of macrophage subtypes. (B) Differences in the proportions of macrophage subtypes between HCC and control tissues. (C) PANoptosis scores of macrophage subtypes. (D-E) Pseudotime analysis of macrophages. (F) Pseudotime gene heatmap of dynamic gene changes in macrophages. (G) Expression differences of transcription factors in macrophage subtypes.

Heterogeneity and functional characterization of CAF subpopulations in the TME of HCC

The heterogeneity of CAFs and their roles in HCC progression are critical. Through secondary clustering analysis, we identified six distinct CAF subpopulations: MT+ CAFs, Ig+ CAFs, mCAFs, iCAFs, pCAFs, and APO+ CAFs (Fig. 5A). In HCC samples, the proportions of inflammatory and stromal CAFs were significantly elevated, closely correlating with their roles in promoting inflammatory cascades and matrix remodeling within the TME (Fig. 5B). PANoptosis score analysis revealed that APO+ CAFs exhibited the highest scores. APO+ CAFs showed elevated expression of lipid-associated protein family genes, consistent with the observed promotion of HCC metabolism, suggesting that these CAFs may regulate PANoptosis through lipid metabolic pathways, thereby driving tumor progression (Fig. 5C). Intercellular Communication analysis further unveiled a complex interaction network among CAF subpopulations. mCAFs, MT+ CAFs, and pCAFs were identified as key communicative nodes, with APO+ CAFs primarily receiving signals from these subgroups (Fig. 5D-E). This suggests that APO+ CAFs may be regulated by other CAF subpopulations. Specifically, APO+ CAF predominantly outputs THBS, VTN, ESAM, and PARs signals, while receiving PTN and ESAM signals (Fig. 5F). Cytotrace analysis of cellular stemness revealed that mCAFs are at an early stage of differentiation, exhibiting the strongest stemness potential, whereas iCAFs and Ig+ CAF are at a later stage of differentiation with lower stemness potential (Fig. 5G-I). This phenomenon aligns with the chronic inflammation characteristic of late-stage tumors. This study provides an in-depth understanding of the heterogeneity and functional characteristics of CAF subpopulations in HCC, while mapping their interaction network. These findings offer new insights into the role of CAFs in HCC progression and present potential directions for the development of targeted therapeutic strategies. Notably, the unique role of APO+ CAFs in PANoptosis and lipid metabolism highlights it as an important therapeutic target for future HCC treatment.

Heterogeneity and metabolic characteristics of EC subpopulations in the TME of HCC

Through clustering analysis, we identified seven subpopulations of ECs: Tip-like ECs, Capillary ECs, MT+ ECs, APO+ ECs, MHCII+ ECs, mECs, and lymphatic ECs (Fig. 6A). In HCC tumor tissues, the proportions of EC subpopulations significantly changed: the increase in Tip-like ECs and MT+ ECs suggests active tumor angiogenesis, while the decrease in Capillary ECs and APO+ ECs indicates alterations in microvascular structures (Fig. 6B). The PANoptosis score for ECs was highest in APO+ ECs, highlighting the significant role of lipid

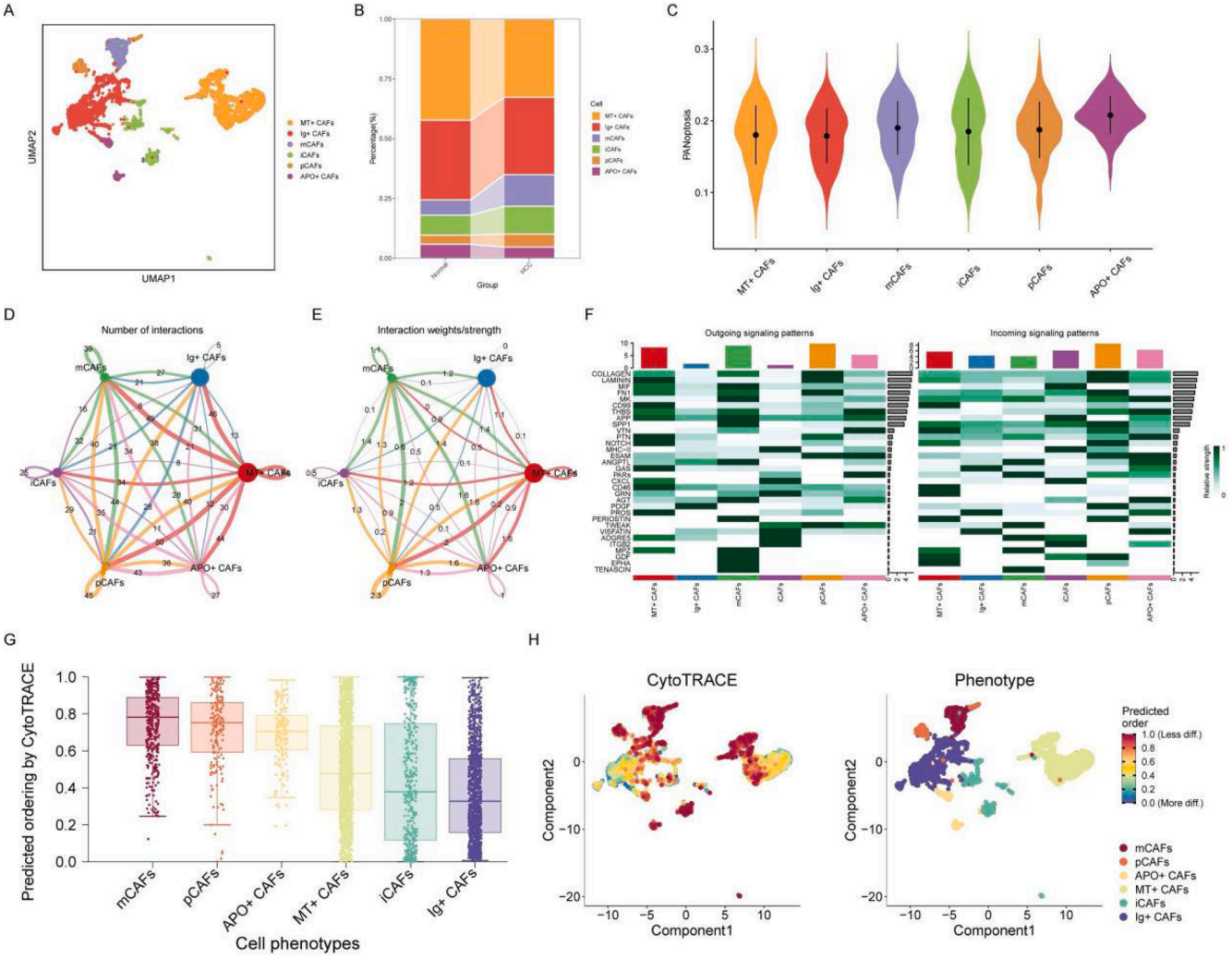

Fig. 5. Overview of major fibroblast subtypes.(A) UMAP plot of cancer-associated fibroblast (CAF) subtypes. (B) Differences in the proportions of CAF subtypes between HCC and control tissues. (C) PANoptosis scores of CAF subtypes. (D-E) Cell communication among CAF subtypes. (F) Relative strength of main signal outputs and inputs by CAFs. (G) Stemness scores of different CAF subtypes, indicating their potential for tumorigenesis. (H) UMAP plot of stemness scores and phenotypes of different CAF subtypes.

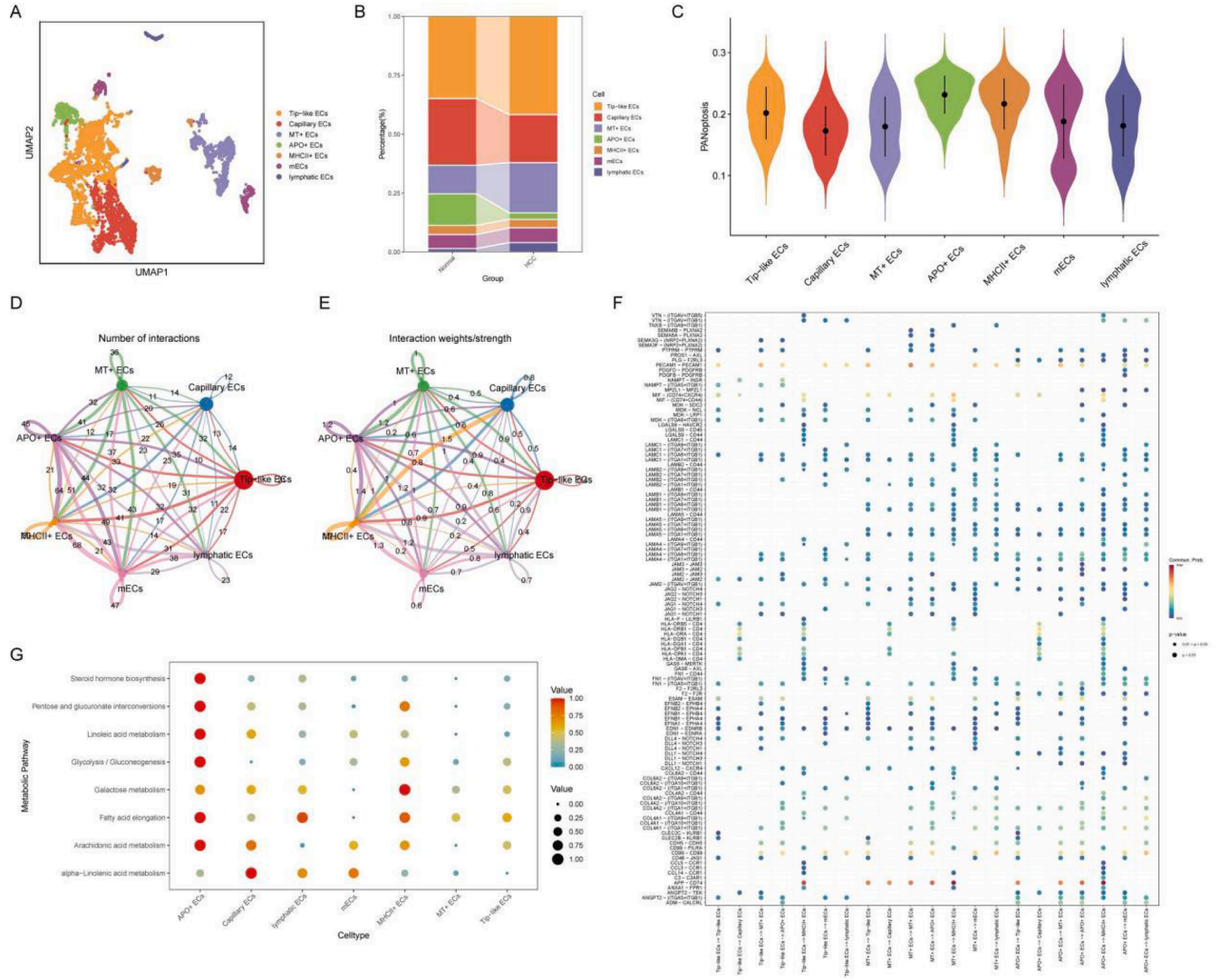

Fig. 6. Overview of major endothelial cell subtypes. (A) UMAP plot of endothelial cell (EC) subgroups. (B) Differences in the proportions of EC subtypes between HCC and control tissues. (C) PANoptosis scores of different EC subgroups. (D-E) Cell communication among different EC subgroups. (F) Analysis of ligand-receptor pairs among different EC subgroups, illustrating intercellular communication. (G) Bubble chart of the differences in scores among different metabolic pathways for various EC subgroups.

metabolism in PANoptosis (Fig. 6C). Intercellular communication analysis revealed that Tip-like ECs, APO+ ECs, mECs, and MT+ ECs exhibited higher communication activity, with APO+ ECs having a substantial communication weight overall (Fig. 6D-E). Ligand-receptor interaction analysis indicated that PECAM1-PECAM1, MIF-(CD74+CXCR4), MIF-(CD74+CD44), and APP-CD74 had the highest communication probabilities, with APP-CD74 serving as the primary communication pathway between APO+ ECs and other EC subpopulations (Fig. 6F). Consistent with the high expression of genes in APO+ ECs, metabolic analysis demonstrated a significant upregulation of carbohydrate and lipid metabolism (Fig. 6G), confirming the role of APO+ ECs in regulating these metabolic processes and providing insights into tumor angiogenesis and metabolic reprogramming. Our analysis comprehensively illustrates the heterogeneity, functional characteristics, and interaction networks of EC subpopulations in HCC. Notably, the unique roles of APO+ ECs in PANoptosis, cell communication, and metabolic reprogramming offer new perspectives on the molecular mechanisms of tumor angiogenesis. These findings enhance our understanding of the HCC and provide potential targets for developing therapeutic strategies against tumor vasculature.

Clinical significance of PANoptosis-Related cell subpopulations in HCC

To assess the clinical significance of PANoptosis-related cell subpopulations identified at the single-cell level, we performed deconvolution analysis of the abundances of Ig+ hepatocytes, MMP12+ macrophages, APO+ CAFs, and APO+ ECs based on their characteristic genes. We examined the relationship between these cell abundances and clinical features in the TCGA-LIHC cohort. Survival analysis revealed that only the abundance of APO+ ECs was significantly associated with overall survival time. Patients with a high abundance of APO+ ECs exhibited better survival outcomes (Fig. 7A-D), suggesting that the activation of PANoptosis in endothelial cells may favor patient survival, providing new insights into the role of tumor vasculature in HCC progression. In terms of histological grading, the abundances of APO+ CAFs and APO+ ECs were closely correlated with tumor differentiation, while Ig+ hepatocytes and MMP12+ macrophages showed no significant association. Lower abundances of APO+ CAFs or APO+ ECs were significantly linked to poorer histological grades (G3/G4) (Fig. 7E-H), indicating their importance in maintaining tumor differentiation. Regarding tumor staging, similar to histological grades, lower abundances of APO+ CAFs or APO+ ECs were significantly associated with

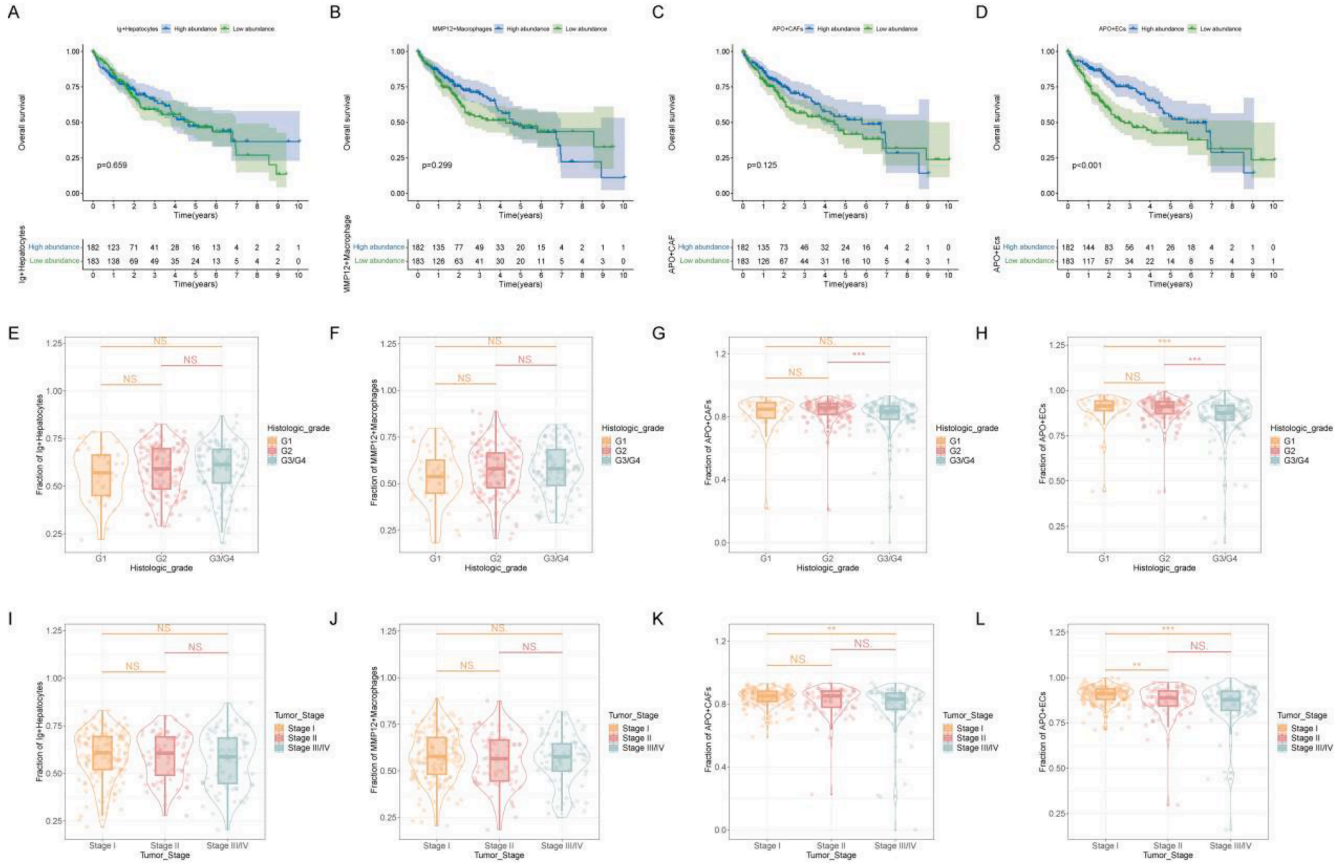

Fig. 7. Association of PANoptosis Activation with Clinical Staging and Prognosis. (A-D) Survival curves relating the abundance of immunoglobulin-positive (Ig+) hepatocytes, matrix metalloproteinase-12 positive (MMP12+) macrophages, apolipoprotein-positive (APO+) CAFs, and APO+ ECs to patient survival rates. (E-H) Correlation analysis between the abundance of Ig+ hepatocytes, MMP12+ macrophages, APO+ CAFs, and APO+ ECs and the histological staging of patients. (I-L) Correlation analysis between the abundance of Ig+ hepatocytes, MMP12+ macrophages, APO+ CAFs, and APO+ ECs and the oncological staging of patients.

higher tumor stages (Stage III/IV) (Fig. 7I-L), suggesting a potential inhibitory role for these cells in HCC progression. These results highlight the unique importance of APO+ ECs in HCC progression and prognosis. Specifically, the activation of PANoptosis in APO+ ECs may inhibit tumor progression, with their abundance closely related to better clinical staging and survival outcomes. In contrast, although the abundance of APO+ CAFs does not directly influence overall survival, it is closely related to tumor grades and staging. Meanwhile, the abundances of Ig+ hepatocytes and MMP12+ macrophages showed no significant correlation with clinical manifestations in HCC patients.

Relationship between PANoptosis-Related cell subpopulations and immunotherapy

To explore the relationship between the abundance of PANoptosis-related cell subpopulations and immunotherapy, we first performed deconvolution analysis of bulk RNA data to obtain the cell abundances of four PANoptosis-related subpopulations and assessed their correlation with cytokine expression. The results indicated that an increase in the abundance of Ig+ hepatocytes and MMP12+ macrophages was associated with a significant upregulation of chemokines and TNF family molecules. Conversely, the abundances of APO+ CAFs and APO+ ECs showed a negative correlation with cytokine expression, with higher abundances of APO+ CAFs and APO+ ECs correlating with decreased chemokine and TNF family expression (Fig. 8A-B). Subsequently, we utilized the TIDE algorithm to further evaluate the association between these cell subpopulations and response to immune checkpoint inhibitor therapy. With the exception of APO+ CAFs, lower abundances of Ig+ hepatocytes, MMP12+ macrophages, and APO+ ECs were linked to lower TIDE scores, suggesting that patients with lower abundances of these cell subpopulations may be more suitable for immunotherapy (Fig. 8C-F). These findings have significant clinical implications, providing new biomarkers for identifying patient populations that may benefit from immunotherapy, revealing the potential regulatory roles of cell subpopulations within the TME on immune responses, and offering new insights into the heterogeneity of immune therapy responses.

Potential mechanisms between high abundance of APO+ ECs and improved clinical outcomes

Based on the analysis of cell abundance and its impact on clinical features and immunotherapy, APO+ ECs are identified as the cell subpopulation most closely associated with clinical outcomes in HCC patients among the four PANoptosis-related subpopulations. To further explore the potential mechanisms underlying the association between high abundance of APO+ ECs and improved survival prognosis and clinical staging, we first reintegrated the different subtypes of ECs into the initial single-cell clustering analysis to investigate the interactions between APO+ ECs and other cell types. Through the analysis of intercellular communication networks, we found that APO+ ECs had the highest communication frequency with fibroblasts, monocytes and macrophages (Fig. 9A-B). In these communication pathways, APO+ ECs primarily transmit signals via MPZ and TWEAK pathways, which are closely related to the proliferation and differentiation of fibroblasts (Fig. 9C). Further analysis showed that in the output pathway interaction receptor scoring, APO+ ECs exhibited the highest interaction receptor scores with T cells, including members of the HLA protein family (Fig. 9D), suggesting that APO+ ECs may play a role in T cell activation.

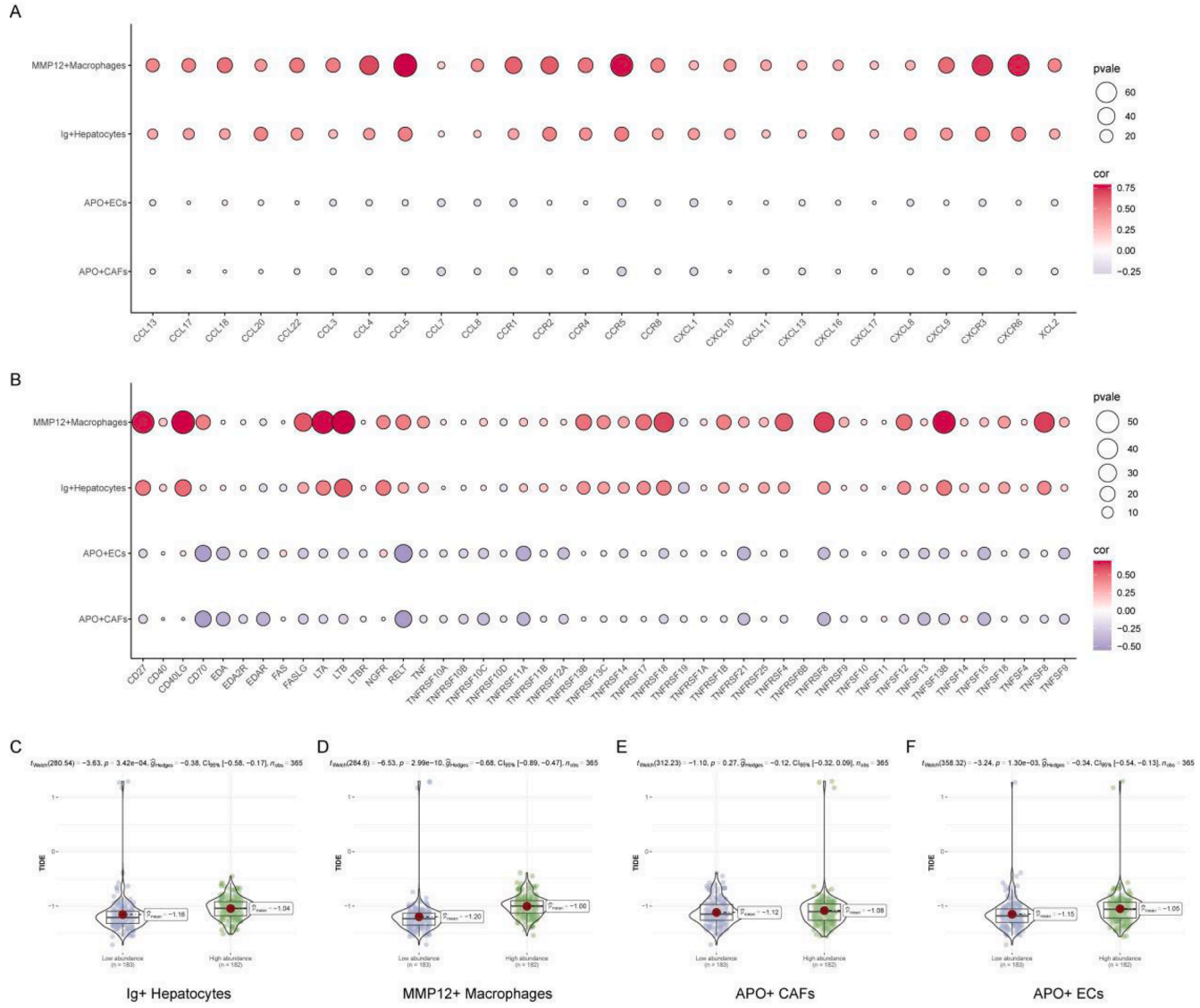

Fig. 8. Association of PANoptosis Activation with Immunotherapy. (A) Analysis of the correlation between the abundance of Ig+ hepatocytes, MMP12+ macrophages, APO+ CAFs, and APO+ ECs and the expression of chemokines, which are signaling molecules involved in immune cell recruitment. (B) Analysis of the correlation between the abundance of Ig+ hepatocytes, MMP12+ macrophages, APO+ CAFs, and APO+ ECs and the expression of tumor necrosis factor (TNF) family molecules. (C-F) Analysis of the correlation between the abundance of Ig+ hepatocytes, MMP12+ macrophages, APO+ CAFs, and APO+ ECs and Tumor Immune Dysfunction and Exclusion (TIDE) scores, a method for predicting response to immunotherapy.

In addition to macrophages and B cells, ECs and fibroblasts can also partially fulfill antigen-presenting functions, which explains the association between the high abundance of APO+ ECs and better survival prognosis as well as clinical staging. In the input pathway receptor analysis of APO+ ECs, T cells and NK cells exhibited the highest regulatory scores for APO+ ECs, further confirming the interactivity of intercellular communication (Fig. 9E).

Mechanism of APO+ ECs in enhancing T cell function

Given the interaction between APO+ ECs and T cells, which suggests a potential immune regulatory function, we conducted a functional analysis to explore whether APO+ ECs could enhance T cell function. In the differential analysis between APO+ ECs and other cells, we identified the top 10 upregulated and downregulated genes in APO+ ECs (Fig. 10A). Enrichment analysis of these differential genes revealed two main categories of upregulated functions in APO+ ECs: one related to immune responses, primarily involving enhanced T cell proliferation and differentiation; the other related to developmental processes, including mesenchymal development, angiogenesis, and maturation. These findings suggest that APO+ ECs may promote favorable outcomes in HCC through these mechanisms (Fig. 10B-C). To further validate the functional interactions between APO+ ECs and T cells, we analyzed the correlation between the deconvolution proportion of APO+ ECs and the expression of HLA family genes. The analysis was consistent with previous studies, showing a significant positive correlation between APO+ ECs and the expression of HLA family molecules, including HLA−*J*, HLA−DQB2, HLA−DQA2, HLA−DQA1, HLA−DPB2, HLA−DOA, and HLA−DMB (Fig. 10D). This indicates that APO+ ECs might influence T cell function by regulating HLA molecule expression. Finally, we explored whether the representative marker genes of APO+ ECs have the potential for disease stratification, selecting the top 20 genes of APO+ ECs for analysis. Using GENEMANIA, we found that these genes primarily involve predictive and physical interaction relationships (Fig. 10E). Stratifying HCC patients based on these 20 genes, we observed a clear division into two subgroups, with significant differences in characteristics shown in principal component analysis (PCA) (Fig. 10F-G). Additionally, patients in Cluster 1 exhibited significantly

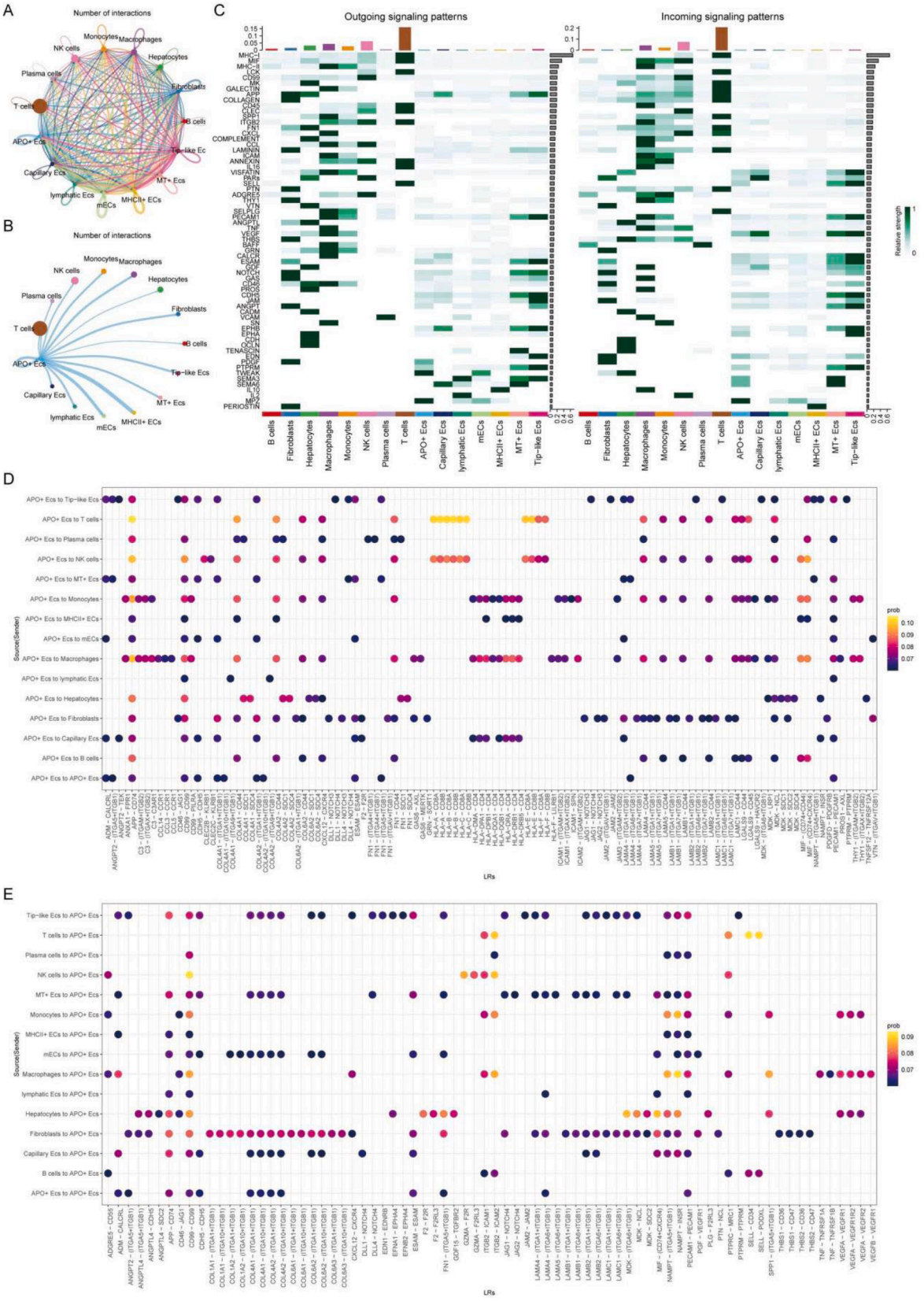

Fig. 9. Cellular Interactions and Immune Signatures Associated with APO+ ECs. (A) Analysis of interactions between APO+ ECs and other cell types. (B) Communication patterns between APO+ ECs and other cell types. (C) Relative strength of main signals output and input by APO+ ECs. (D-E) Analysis of incoming and outgoing receptor-ligand interactions of APO+ ECs, detailing how they communicate with other cell types via specific proteins.

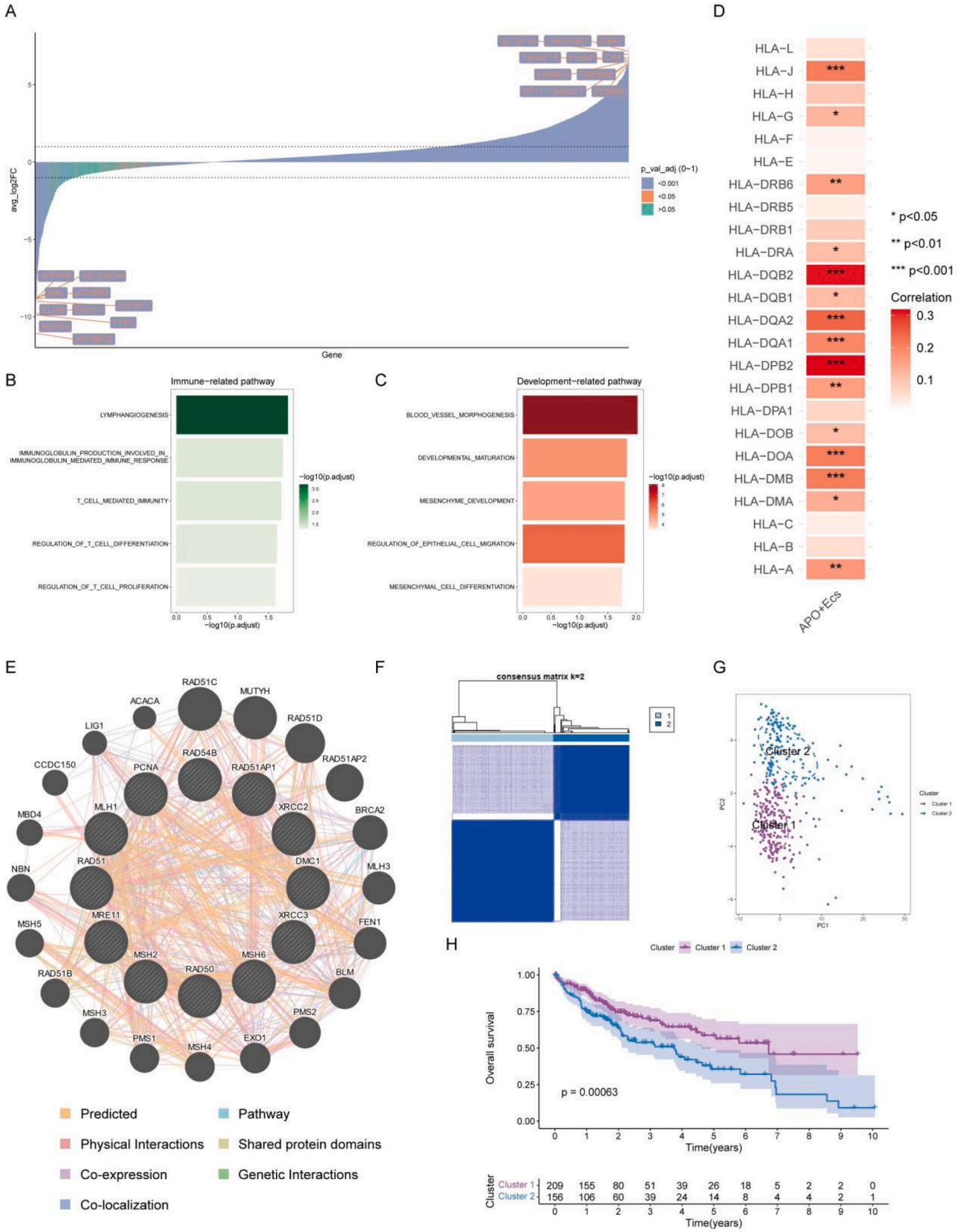

Fig. 10. The clinical significance of APO+ ECs related to T cells. (A) Differential gene expression in APO+ ECs. (B-C) Enrichment analysis of differential genes in APO+ ECs. (D) Correlation analysis between APO+ ECs and human leukocyte antigen (HLA) family genes, which play a role in immune response. (E) Gene interaction network of APO+ ECs. (F) Patient stratification based on APO+ ECs gene expression. (G) Principal component analysis (PCA) of patient clusters, which visualizes the relationships between different groups based on gene expression profiles. (H) Survival analysis of patient clusters based on APO+ ECs gene expression.

better survival rates, indicating that the representative genes of APO+ ECs could serve not only as biomarkers for disease stratification but also as potential guides for prognosis (Fig. 10H).

The APO family demonstrates enhanced co-localization in pericancerous tissues and suppresses the proliferative capacity of hepatocellular carcinoma cells via co-culture

The PANoptosis scoring analysis of the APO family endothelial cells revealed that the top three endothelial cell subpopulations are APOH+ ECs, TTR+ ECs, and RGCC+ ECs. IF results indicated that these three EC subpopulations are significantly enriched in the adjacent tissues of HCC patients, while being relatively sparse in tumor tissues (Fig. 11A-C). This phenomenon suggests that APOH+ ECs, TTR+ ECs, and RGCC+ ECs may play a critical role in the progression of HCC, and the reduction in the abundance of these cell subpopulations may be closely associated with the development of HCC. Analysis of single-cell sequencing data revealed that the presence of APOH+ ECs is significantly associated with favorable prognosis and immune therapy outcomes in HCC patients. To further validate this finding, we transfected OE-APOH plasmid into HUVEC and co-cultured them with HCCLM3 and Huh7 cells using Transwell chambers (Fig. 11D-E). After 48 hours of co-culture, CCK8 assays showed that APOH+ HUVECs significantly inhibited the proliferation of both HCCLM3 and Huh7 cells (Fig. 11F-G).

Discussion

The interaction between tumor cells and various immune cells in the tumor microenvironment (TME) is crucial for the development and progression of cancer. Immune cells crosstalk with tumor cells by secreting various factors to help shape this process [24–26]. Previous studies have shown that single-cell RNA sequencing (scRNA-seq) exhibits excellent capabilities in assessing the TME, enabling the depiction of the complex immune landscape and intercellular interactions present in human HCC. Tang W et al. [27] analyzed the immune landscape of 15 samples from patients with stage III and IV liver cancer using scRNA-seq technology and found that FABP1 is overexpressed in tumor-associated macrophages (TAMs) in stage III HCC tissues, promoting immune escape in HCC through interaction with PPARG/CD36 in TAMs. These findings contribute to a deeper understanding of the immune escape mechanisms associated with tumor recurrence. No studies have investigated the relationship between PANoptosis and the TME associated with HCC using scRNA-seq. In the current study, we conducted a deep analysis by integrating three GEO single-cell datasets (GSE149614, GSE166635, GSE189903), revealing multiple immune cell subtypes significantly associated with PANoptosis, including (Ig+ hepatocytes, MMP12+ macrophages, APO+ CAFs, APO+ ECs), and describing the developmental pathways followed by different cell types. Additionally, we paid special attention to the APO+ ECs subtype and conducted a more detailed exploration. Our study provides rich data and theoretical basis for the development of HCC.

Apolipoprotein E (APOE) is a ligand that binds to various liver receptors, typically promoting lipid accumulation by increasing the uptake of high-density lipoprotein (HDL). This process exacerbates the progression of fatty liver and liver disease [28–30], and also leads to the occurrence of HCC by enhancing hepatitis B virus (HBV) infection and replication [31]. Lipid metabolism plays a crucial role in maintaining tumor cell growth. Wang Y et al. [32] showed that APOE is significantly upregulated in microvascular invasion (MVI) of HCC and affects HCC prognosis by increasing lipid metabolism levels, which is consistent with our research results. In addition, Habenicht et al. [33] found that the ApoE-C1q complex is highly expressed in mouse models of hepatitis and hepatocellular carcinoma, as well as in human viral hepatitis and non-alcoholic fatty liver disease. The ApoE-C1q complex can inhibit the classical complement cascade, reduce inflammation, and maintain tissue homeostasis, providing a theoretical basis for the potential mechanism of APOE overexpression in hepatocellular carcinoma [34]. The main function of the apolipoprotein (APO) gene family is to encode apolipoproteins, and dysregulation of these apolipoproteins is closely related to cancer [35]. For example, APOA1 expression is increased in HCC and promotes apoptosis by downregulating the MAPK pathway [36,37]. Lee et al. [38] found that low APOB activity is associated with the upregulation of oncogenic and metastatic regulatory factors such as HGF, MTIF, and ERBB2, as well as the inhibition of tumor suppressor genes TP53 and PTEN. In our study, we conducted an in-depth analysis of four cell subpopulations (Ig+ hepatocytes, MMP12+ macrophages, APO+ CAFs, APO+ ECs) most significantly associated with pan-apoptosis, and used deconvolution algorithms to evaluate the impact of these four cell subpopulations on the clinical prognosis of HCC patients. Notably, only the downregulation of APO+ ECs is associated with poor prognosis and clinical pathological characteristics in HCC patients. Furthermore, the level of APO+ ECs is inversely proportional to chemokines and TNF family molecules, further explaining the key role of APO+ ECs in regulating inflammatory chemotaxis. Immune checkpoint inhibitors (ICIs) are crucial in the treatment of HCC, significantly improving the prognosis of patients with advanced HCC [39,40]. However, immune resistance often occurs during treatment.

In tumor immunotherapy, pro-inflammatory cytokines such as interferon (IFN) and tumor necrosis factor (TNF) can play a double-edged role. Initially, they may enhance the immune response to promote tumor clearance, but subsequently, they can inhibit the immune response through chronic inflammation [41]. For instance, IFN signaling can induce the high expression of interferon-stimulated genes associated with resistance in non-small cell lung cancer and other cancer types [42–44]. The emergence of PD-1/PD-L1 antagonists has shown great potential in improving the prognosis of cancer patients. For example, the PD-1 antibody drug nivolumab injection has demonstrated excellent efficacy in treating melanoma and non-small cell lung cancer, effectively prolonging patient survival [45]. Interestingly, low levels of APO+ ECs are associated with low TIDE scores, indicating that immunotherapy may be an effective target. We further conducted cell communication and enrichment analysis on the APO+ ECs family, revealing that APO+ ECs have the strongest communication intensity with T cells. They may directly interact with T cells by upregulating HLA molecule expression, enhancing the antigen presentation function of T cells and NK cells. Previous studies have shown that endothelial cells can activate CD4+ *T* cells through HLA-DR, supporting our findings [46]. It has been shown that in HCC, fatty acids are converted into acetyl-CoA through fatty acid β-oxidation, which then provides energy support for the proliferation and metastasis of tumor cells via oxidative phosphorylation [47]. However, in ECs, acetyl-CoA produced from fatty acid β-oxidation is primarily used to combine with carbon donor substrates, promoting the synthesis of deoxyribonucleotide triphosphates, thus providing the essential material basis for DNA synthesis in ECs, a process that is crucial for cell proliferation and repair [48]. It is worth noting that functional analysis results indicate a significant upregulation of lipid and glucose metabolism in APO+ ECs. This suggests that APO+ ECs may influence the proliferation of HCC cells by regulating the uptake of fatty acids, their oxidation, and the generation of metabolic products. Additionally, ligand-receptor pair analysis of endothelial cells revealed a significant upregulation in the frequency of APP-CD74 communication. Furthermore, using immunofluorescence technology, we found that the APO+ ECs family (ECs-APOH, ECs-TTR, ECs-RGCC) has more co-localization with endothelial cells in adjacent tissues compared to liver cancer tissues. Next, we chose to overexpress the APOH gene in human endothelial cells (HUVEC) and co-cultured the transfected HUVEC cells with liver cancer Huh-7 and HCCLM3 cells in upper and lower layers using transwell chambers. The results showed that co-cultured Huh-7 and HCCLM3 cells exhibited significant proliferation inhibition compared to non-co-cultured Huh-7 and HCCLM3 cells. Therefore, we speculate that the regulation of APO+ ECs family gene expression in endothelial cells through this ligand-receptor interaction plays a significant role in

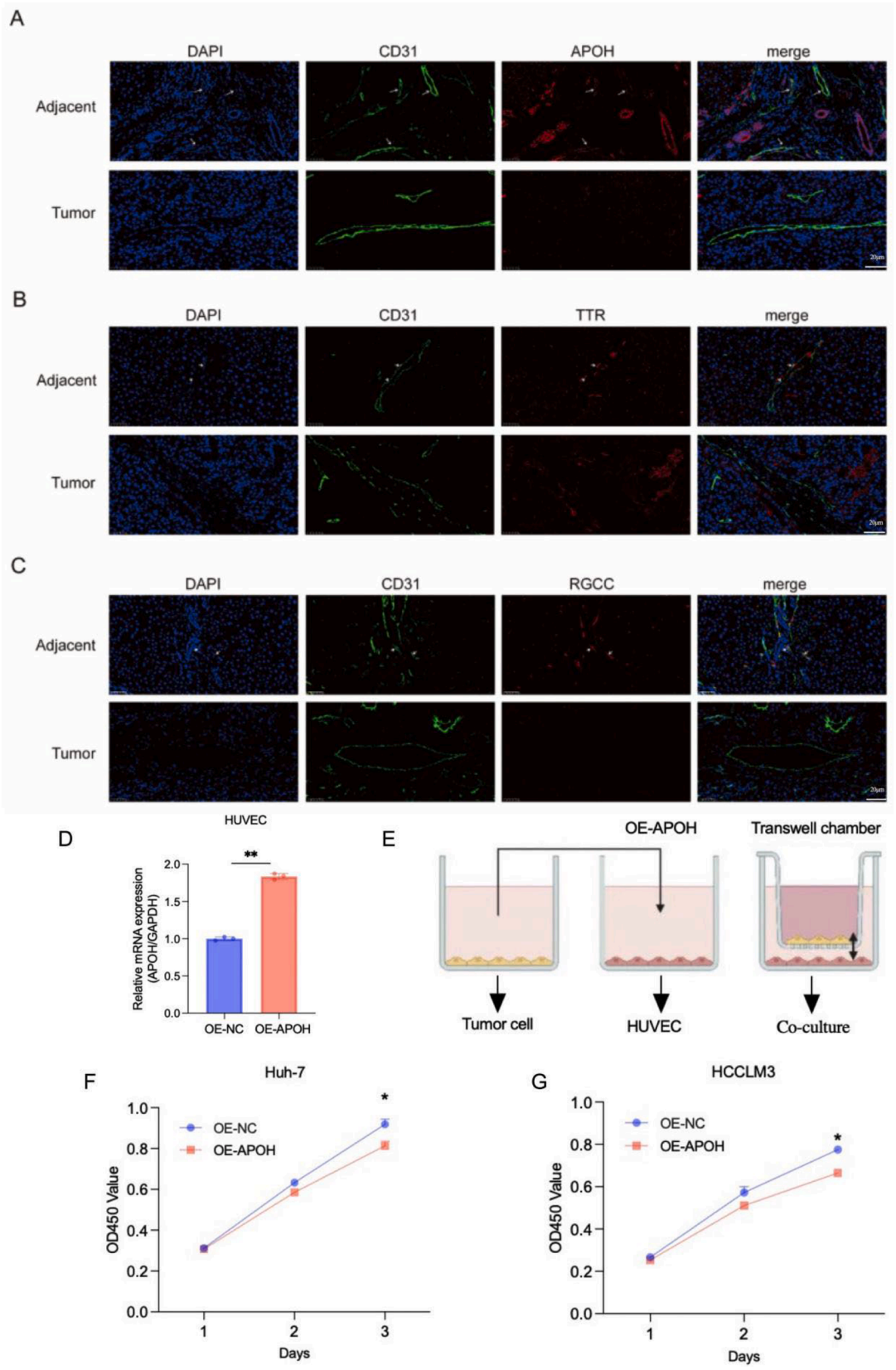

Fig. 11. Expression differences of APO+ ECs in tumor tissues and tumor border tissues using immunofluorescence (IF) staining. (A-C) Expression differences of the top three genes of the APO family in APO+ ECs with differential expression folds (APOH, TTR, and RGCC) in tumor tissues and adjacent tissues, respectively, observed using IF staining. (D) Quantitative reverse-transcription polymerase chain reaction (qRT-PCR) detection of APOH expression in human umbilical vein endothelial cells (HUVECs). (E) Construction of co-culture conditions. (F-G) CCK-8 assay to detect the proliferation of HCC Huh-7 and HCCLM3 cells after co-culture with APO+ ECs.

improving the prognosis of liver cancer patients.

In summary, we utilized single-cell sequencing technology to establish the single-cell tumor heterogeneity landscape of HCC and revealed four cell subtype classifications most closely related to PANoptosis. Among them, the decrease in the abundance of APO+ECs closely related to PANoptosis is an important factor for poor prognosis in liver cancer. Cell communication technology further revealed the interaction pathways between tumor cells and endothelial cells. Compared with HCC tissues, there are more APO+ECs family localizations in normal tissues, which was fully confirmed by immunofluorescence detection. In vitro experiments also showed that endothelial cells may inhibit the growth of liver cancer cells by upregulating the APOH gene, which is a promising therapeutic target for improving the prognosis of liver cancer patients. Our study provides previously unknown insights into the tumor heterogeneity of HCC and identifies its potential mechanisms of action. Based on the findings of this study, we believe that members of the APO family may play a significant role in the development of HCC. Therefore, future research could consider the APO family as potential biomarkers or therapeutic targets. In clinical applications, the expression levels of APO family members could serve as stratification factors to assess the efficacy of different treatment regimens (such as immunotherapy or targeted therapy) for HCC patients. By analyzing the dynamic changes in APO family members in the tumor microenvironment, and incorporating molecular marker detection, more scientifically grounded and precise treatment plans could be developed for patients.

Conclusion

This study systematically mapped the cellular landscape of the TME in HCC patients, with a focus on subpopulations exhibiting high PANoptosis scores, including ECs, macrophages, hepatocytes, and fibroblasts. We further explored the differences in their developmental trajectories, metabolic pathways, and gene expression profiles. Additionally, we elucidated the potential molecular mechanisms by which APO+ ECs regulate cell communication within the TME, thereby inhibiting HCC cell proliferation, improving prognosis, and enhancing the efficacy of immunotherapy. This research provides novel insights into clinical prognosis evaluation and offers potential targets for immunotherapeutic strategies in HCC.

Abbreviations

HCC, hepatocellular carcinoma; PCD, programmed cell death; TNF, tumor necrosis factor; IFN-γ, interferon-gamma; TME, Tumor microenvironment; TAM, tumor-associated macrophage; CAF, cancer-associated fibroblast; EC, endothelial cell; scRNA-seq, single-cell RNA sequencing; GEO, Gene Expression Omnibus database; TCGA, The Cancer Genome Atlas database; IF, immunofluorescence staining; FFPE, formalin-fixed paraffin-embedded tissues; PBS, phosphate-buffered saline; HLA, human leukocyte antigen; PCA, principal component analysis; APO, apolipoprotein; APP, amyloid precursor protein.

Funding

None.

Author contributions

Xiushen Li was involved in the conceptualization of the study, formal analysis, and drafting the manuscript. Xiangyu Yang contributed to the methodology, data collection, and statistical analysis. Yi Ren provided critical support in data curation and revision of the manuscript.Qi Zhang, Sailing Lin, Wenhao Wu, Xiaolu Yang, Jiahan Zheng and Xinzhu Liu provided valuable feedback for manuscript refinement. Zhaorui Cheng and Xiaoyong Chen and Yuxin Qian supervised the entire project, contributed to the manuscript editing, and provided key intellectual input.

Data Availability

The raw data utilized in this study was sourced from a publicly accessible data platform. The liver cancer sample dataset was obtained from TCGA (http://portal.gdc.cancer.gov). For the single-cell dataset, its accession number is GSE149614 (10 HCC patients), GSE166635 (2 HCC patients), and GSE189903 (4 HCC patients), and the pertinent data can be accessed through the following link: (https://www.ncbi.nlm.nih.gov/).

Ethics aproval and consent to participate

This study was approved by the ethics committee of The Second Affiliated Hospital of Nanchang University (approval no.O-2024,147) and Natural Science Foundation of Jiangxi Province (20192BAB205112). We certify that the study was performed in accorgence1964 declaration of HELSINKI and later amendments.

Consent to participate

Not applicable.

Consent to publish

Not applicable.

CRediT authorship contribution statement

Zhaorui Cheng: Methodology, Investigation, Data curation. **Xiangyu Yang:** Conceptualization. **Yi Ren:** Writing – review & editing, Writing – original draft. **Huimin Wang:** Data curation. **Qi Zhang:** Data curation. **Sailing Lin:** Conceptualization. **Wenhao Wu:** Conceptualization. **Xiaolu Yang:** Conceptualization. **Jiahan Zheng:** Formal analysis. **Xinzhu Liu:** Data curation. **Xin Tao:** Investigation. **Xiaoyong Chen:** Conceptualization. **Yuxin Qian:** Investigation. **Xiushen Li:** Formal analysis, Data curation, Conceptualization.

Declaration of competing interest

The authors declare that there are no competing interests.

Acknowledgements

None

Supplementary materials

Supplementary material associated with this article can be found, in the online version, at doi:10.1016/j.tranon.2025.102402.

References

[1] H. Rumgay, J. Ferlay, C. de Martel, et al., Global, regional and national burden of primary liver cancer by subtype, Eur. J. Cancer 161 (2022) 108–118, https://doi.org/10.1016/j.ejca.2021.11.023.
[2] A. Forner, M. Reig, J. Bruix, Hepatocellular carcinoma, Lancet 391 (10127) (2018) 1301–1314, https://doi.org/10.1016/S0140-6736(18)30010-2.
[3] A.G. Singal, J.M. Llovet, M. Yarchoan, et al., AASLD Practice guidance on prevention, diagnosis, and treatment of hepatocellular carcinoma, Hepatology 78 (6) (2023) 1922–1965, https://doi.org/10.1097/HEP.0000000000000466.
[4] Liver EAftSot. EASL Clinical Practice Guidelines: management of hepatocellular carcinoma, J. Hepatol. 69 (1) (2018) 182–236, https://doi.org/10.1016/j.jhep.2018.03.019.
[5] J.M. Llovet, R. Pinyol, M. Yarchoan, et al., Adjuvant and neoadjuvant immunotherapies in hepatocellular carcinoma, Nat. Rev. Clin. Oncol. 21 (4) (2024) 294–311, https://doi.org/10.1038/s41571-024-00868-0.
[6] B. Sangro, P. Sarobe, S. Hervás-Stubbs, I. Melero, Advances in immunotherapy for hepatocellular carcinoma, Nat. Rev. Gastroenterol. Hepatol. 18 (8) (2021) 525–543, https://doi.org/10.1038/s41575-021-00438-0.

[7] A. Pandeya, T.D. Kanneganti, Therapeutic potential of PANoptosis: innate sensors, inflammasomes, and RIPKs in PANoptosomes, Trends. Mol. Med. 30 (1) (2024) 74–88, https://doi.org/10.1016/j.molmed.2023.10.001.
[8] Karki R., Sharma B.R., Tuladhar S., et al. Synergism of TNF-α and IFN-γ triggers inflammatory cell death, tissue damage, and mortality in SARS-CoV-2 infection and Cytokine shock syndromes. Cell. 2021;184(1)doi:10.1016/j.cell.2020.11.025.
[9] D.K.W. Ocansey, F. Qian, P. Cai, et al., Current evidence and therapeutic implication of PANoptosis in cancer, Theranostics 14 (2) (2024) 640–661, https://doi.org/10.7150/thno.91814.
[10] Z. Liu, L. Sun, X. Peng, et al., PANoptosis subtypes predict prognosis and immune efficacy in gastric cancer, Apoptosis 29 (5–6) (2024) 799–815, https://doi.org/10.1007/s10495-023-01931-4.
[11] X. Wang, R. Sun, S. Chan, et al., PANoptosis-based molecular clustering and prognostic signature predicts patient survival and immune landscape in colon cancer, Front. Genet. 13 (2022) 955355, https://doi.org/10.3389/fgene.2022.955355.
[12] Y. Cai, H. Xiao, S. Xue, et al., Integrative analysis of immunogenic PANoptosis and experimental validation of cinobufagin-induced activation to enhance glioma immunotherapy, J. Exp. Clin. Cancer Res. 44 (1) (2025) 35, https://doi.org/10.1186/s13046-025-03301-1.
[13] J. Wang, Y. Chen, Y. Xu, et al., DNASE1L3-mediated PANoptosis enhances the efficacy of combination therapy for advanced hepatocellular carcinoma, Theranostics 14 (17) (2024) 6798–6817, https://doi.org/10.7150/thno.102995.
[14] K.Y. Shen, Y. Zhu, S.Z. Xie, L.X. Qin, Immunosuppressive tumor microenvironment and immunotherapy of hepatocellular carcinoma: current status and prospectives, J. Hematol. Oncol. 17 (1) (2024) 25, https://doi.org/10.1186/s13045-024-01549-2.
[15] E. Güç, J.W. Pollard, Redefining macrophage and neutrophil biology in the metastatic cascade, Immunity 54 (5) (2021) 885–902, https://doi.org/10.1016/j.immuni.2021.03.022.
[16] E. Sahai, I. Astsaturov, E. Cukierman, et al., A framework for advancing our understanding of cancer-associated fibroblasts, Nat. Rev. Cancer 20 (3) (2020) 174–186, https://doi.org/10.1038/s41568-019-0238-1.
[17] M. De Palma, D. Biziato, T.V. Petrova, Microenvironmental regulation of tumour angiogenesis, Nat. Rev. Cancer 17 (8) (2017) 457–474, https://doi.org/10.1038/nrc.2017.51.
[18] K.E. de Visser, J.A. Joyce, The evolving tumor microenvironment: from cancer initiation to metastatic outgrowth, Cancer Cell 41 (3) (2023) 374–403, https://doi.org/10.1016/j.ccell.2023.02.016.
[19] A. Mantovani, P. Allavena, F. Marchesi, C. Garlanda, Macrophages as tools and targets in cancer therapy, Nat. Rev. Drug Discov. 21 (11) (2022) 799–820, https://doi.org/10.1038/s41573-022-00520-5.
[20] B. Cogliati, C.N. Yashaswini, S. Wang, D. Sia, S.L. Friedman, Friend or foe? The elusive role of hepatic stellate cells in liver cancer, Nat. Rev. Gastroenterol. Hepatol. 20 (10) (2023) 647–661, https://doi.org/10.1038/s41575-023-00821-z.
[21] Q. Zeng, M. Mousa, A.S. Nadukkandy, et al., Understanding tumour endothelial cell heterogeneity and function from single-cell omics, Nat. Rev. Cancer 23 (8) (2023) 544–564, https://doi.org/10.1038/s41568-023-00591-5.
[22] X. Yi, J. Li, X. Zheng, et al., Construction of PANoptosis signature: novel target discovery for prostate cancer immunotherapy, Mol. Ther. Nucleic. Acids. 33 (2023) 376–390, https://doi.org/10.1016/j.omtn.2023.07.010.
[23] F. Song, C.G. Wang, J.Z. Mao, et al., PANoptosis-based molecular subtyping and HPAN-index predicts therapeutic response and survival in hepatocellular carcinoma, Front. Immunol. 14 (2023) 1197152, https://doi.org/10.3389/fimmu.2023.1197152.
[24] D. Hanahan, R.A. Weinberg, Hallmarks of cancer: the next generation, Cell 144 (5) (2011) 646–674, https://doi.org/10.1016/j.cell.2011.02.013.
[25] L. Bejarano, M.J.C. Jordão, J.A. Joyce, Therapeutic targeting of the tumor microenvironment, Cancer Discov. 11 (4) (2021) 933–959, https://doi.org/10.1158/2159-8290.CD-20-1808.
[26] P. Sharma, A. Aaroe, J. Liang, V.K. Puduvalli, Tumor microenvironment in glioblastoma: current and emerging concepts, Neurooncol. Adv. 5 (1) (2023) vdad009, https://doi.org/10.1093/noajnl/vdad009.
[27] W. Tang, G. Sun, G.W. Ji, et al., Single-cell RNA-sequencing atlas reveals an FABP1-dependent immunosuppressive environment in hepatocellular carcinoma, J. ImmunOther Cancer 11 (11) (2023), https://doi.org/10.1136/jitc-2023-007030.
[28] O. Jamialahmadi, R.M. Mancina, E. Ciociola, et al., Exome-wide association study on alanine aminotransferase identifies sequence variants in the GPAM and APOE associated with fatty liver disease, Gastroenterology 160 (5) (2021), https://doi.org/10.1053/j.gastro.2020.12.023.
[29] N.D. Palmer, B. Kahali, A. Kuppa, et al., Allele-specific variation at APOE increases nonalcoholic fatty liver disease and obesity but decreases risk of Alzheimer's disease and myocardial infarction, Hum. Mol. Genet. 30 (15) (2021) 1443–1456, https://doi.org/10.1093/hmg/ddab096.
[30] A.M. Morton, M. Koch, C.O. Mendivil, et al., Apolipoproteins E and CIII interact to regulate HDL metabolism and coronary heart disease risk, JCI. Insight. 3 (4) (2018), https://doi.org/10.1172/jci.insight.98045.
[31] L. Qiao, G.G. Luo, Human apolipoprotein E promotes hepatitis B virus infection and production, PLoS. Pathog. 15 (8) (2019) e1007874, https://doi.org/10.1371/journal.ppat.1007874.
[32] Y. Wang, G.Q. Zhu, R. Yang, et al., Deciphering intratumoral heterogeneity of hepatocellular carcinoma with microvascular invasion with radiogenomic analysis, J. Transl. Med. 21 (1) (2023) 734, https://doi.org/10.1186/s12967-023-04586-6.
[33] L.K.L. Habenicht, Z. Wang, X. Zhang, et al., The C1q-ApoE complex: a new hallmark pathology of viral hepatitis and nonalcoholic fatty liver disease, Front. Immunol. 13 (2022) 970938, https://doi.org/10.3389/fimmu.2022.970938.
[34] C. Yin, S. Ackermann, Z. Ma, et al., ApoE attenuates unresolvable inflammation by complex formation with activated C1q, Nat. Med. 25 (3) (2019) 496–506, https://doi.org/10.1038/s41591-018-0336-8.
[35] L. Ren, J. Yi, W. Li, et al., Apolipoproteins and cancer, Cancer Med. 8 (16) (2019) 7032–7043, https://doi.org/10.1002/cam4.2587.
[36] D. Bharali, B.D. Banerjee, M. Bharadwaj, S.A. Husain, P. Kar, Expression analysis of apolipoproteins AI & AIV in hepatocellular carcinoma: a protein-based hepatocellular carcinoma-associated study, Indian J. Med. Res. 147 (4) (2018) 361–368, https://doi.org/10.4103/ijmr.IJMR_1358_16.
[37] X.L. Ma, X.H. Gao, Z.J. Gong, et al., Apolipoprotein A1: a novel serum biomarker for predicting the prognosis of hepatocellular carcinoma after curative resection, Oncotarget 7 (43) (2016) 70654–70668, https://doi.org/10.18632/oncotarget.12203.
[38] G. Lee, Y.S. Jeong, D.W. Kim, et al., Clinical significance of APOB inactivation in hepatocellular carcinoma, Exp. Mol. Med. 50 (11) (2018), https://doi.org/10.1038/s12276-018-0174-2.
[39] Y. Zhang, Z. Zhang, The history and advances in cancer immunotherapy: understanding the characteristics of tumor-infiltrating immune cells and their therapeutic implications, Cell Mol. Immunol. 17 (8) (2020) 807–821, https://doi.org/10.1038/s41423-020-0488-6.
[40] J.M. Llovet, F. Castet, M. Heikenwalder, et al., Immunotherapies for hepatocellular carcinoma, Nat. Rev. Clin. Oncol. 19 (3) (2022) 151–172, https://doi.org/10.1038/s41571-021-00573-2.
[41] P. Berraondo, M.F. Sanmamed, M.C. Ochoa, et al., Cytokines in clinical cancer immunotherapy, Br. J. Cancer 120 (1) (2019), https://doi.org/10.1038/s41416-018-0328-y.
[42] J.L. Benci, L.R. Johnson, R. Choa, et al., Opposing functions of interferon coordinate adaptive and innate immune responses to cancer immune checkpoint blockade, Cell 178 (4) (2019), https://doi.org/10.1016/j.cell.2019.07.019.
[43] J. Qiu, B. Xu, D. Ye, et al., Cancer cells resistant to immune checkpoint blockade acquire interferon-associated epigenetic memory to sustain T cell dysfunction, Nat. Cancer 4 (1) (2023) 43–61, https://doi.org/10.1038/s43018-022-00490-y.
[44] D. Memon, A.J. Schoenfeld, D. Ye, et al., Clinical and molecular features of acquired resistance to mmunotherapy in non-small cell lung cancer, Cancer Cell 42 (2) (2024), https://doi.org/10.1016/j.ccell.2023.12.013.
[45] P.M. Forde, J. Spicer, S. Lu, et al., Neoadjuvant Nivolumab plus chemotherapy in resectable lung cancer, N. Engl. J. Med. 386 (21) (2022) 1973–1985, https://doi.org/10.1056/NEJMoa2202170.
[46] F. Galvão, K.C. Grokoski, B.B. da Silva, M.L. Lamers, I.R. Siqueira, The amyloid precursor protein (APP) processing as a biological link between Alzheimer's disease and cancer, Ageing Res. Rev. 49 (2019) 83–91, https://doi.org/10.1016/j.arr.2018.11.007.
[47] Y. Liu, Z. Wu, Y. Li, et al., Metabolic reprogramming and interventions in angiogenesis, J. Adv. Res. 70 (2025) 323–338, https://doi.org/10.1016/j.jare.2024.05.001.
[48] S. Schoors, U. Bruning, R. Missiaen, et al., Fatty acid carbon is essential for dNTP synthesis in endothelial cells, Nature 520 (7546) (2015) 192–197, https://doi.org/10.1038/nature14362.